RADC-TR-90-15
Final Technical Report
March 1990

AD-A221 208

ELECTROMIGRATION IN METALLIC MICROSTRUCTURES

University of Wisconsin at Milwaukee

Richard S. Sorbello

DTIC
ELECTE
MAY 0 4 1990
S E D

APPROVED FOR PUBLIC RELEASE; DISTRIBUTION UNLIMITED.

Rome Air Development Center
Air Force Systems Command
Griffiss Air Force Base, NY 13441-5700

90

This report has been reviewed by the RADC Public Affairs Division (PA) and is releasable to the National Technical Information Services (NTIS) At NTIS it will be releasable to the general public, including foreign nations.
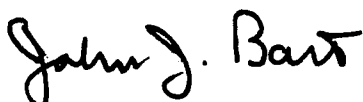
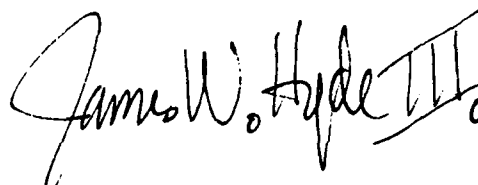RADC-TR-90-15 has been reviewed and is approved for publication.

APPROVED:

MARK W. LEVI
Project Engineer

APPROVED:

JOHN J. BART
Technical Director
Directorate of Reliability & Compatibility

FOR THE COMMANDER:

JAMES W. HYDE III
Directorate of Plans & Programs

If your address has changed or if you wish to be removed from the RADC mailing list, or if the addressee is no longer employed by your organization, please notify RADC (RBRP) Griffiss AFB NY 13441-5700. This will assist us in maintaining a current mailing list.

Do not return copies of this report unless contractual obligations or notices on a specific document require that it be returned.

UNCLASSIFIED

SECURITY CLASSIFICATION OF THIS PAGE

REPORT DOCUMENTATION PAGE		*Form Approved* OMB No. 0704-0188

1a. REPORT SECURITY CLASSIFICATION UNCLASSIFIED		1b RESTRICTIVE MARKINGS N/A	
2a. SECURITY CLASSIFICATION AUTHORITY N/A		3. DISTRIBUTION/AVAILABILITY OF REPORT Approved for public release; distribution unlimited.	
2b. DECLASSIFICATION/DOWNGRADING SCHEDULE N/A			
4. PERFORMING ORGANIZATION REPORT NUMBER(S) N/A		5. MONITORING ORGANIZATION REPORT NUMBER(S) RADC-TR-90-15	
6a. NAME OF PERFORMING ORGANIZATION University of Wisconsin at Milwaukee	6b. OFFICE SYMBOL *(If applicable)*	7a. NAME OF MONITORING ORGANIZATION Rome Air Development Center (RBRP)	
6c. ADDRESS *(City, State, and ZIP Code)* P O Box 413 Milwaukee WI 43201		7b. ADDRESS *(City, State, and ZIP Code)* Griffiss AFB NY 13441-5700	
8a. NAME OF FUNDING/SPONSORING ORGANIZATION AFOSR	8b. OFFICE SYMBOL *(If applicable)*	9. PROCUREMENT INSTRUMENT IDENTIFICATION NUMBER F30602-85-C-0071	

8c. ADDRESS *(City, State, and ZIP Code)* Bolling AFB DC 20332-6448	10. SOURCE OF FUNDING NUMBERS			
	PROGRAM ELEMENT NO. 61102F	PROJECT NO 2306	TASK NO J4	WORK UNIT ACCESSION NO 17

11. TITLE *(Include Security Classification)*

ELECTROMIGRATION IN METALLIC MICROSTRUCTURES

12 PERSONAL AUTHOR(S)
Richard S. Sorbello

13a. TYPE OF REPORT Final	13b. TIME COVERED FROM Jun 85 TO Mar 89	14. DATE OF REPORT *(Year, Month, Day)* March 1990	15 PAGE COUNT 60

16. SUPPLEMENTARY NOTATION

N/A

17. COSATI CODES			18. SUBJECT TERMS *(Continue on reverse if necessary and identify by block number)*
FIELD	GROUP	SUB-GROUP	Electromigration , Thermomigration , crystal
13	08		
20	12		Quantum Mechanics , Mesoscopic Structures ·

19. ABSTRACT *(Continue on reverse if necessary and identify by block number)*

Theoretical studies of electromigration in metallic microstructures have been performed in atomic dynamics and electronic aspects of driving forces. A general formulation of electrical conductivity and electromigration in bulk systems, thin films, and other low-dimensional systems has been constructed. Electromigration driving forces can be calculated from consideration of elastic scattering, although it is the inelastic part of the electron scattering that propels the migrating atom. However, non-adiabatic recoil effects play an important role in the atomic migration of light interstitials at lower temperatures. Model calculations for electromigration at grain boundaries, dislocations and surfaces show substantial variation in driving forces as an interface is approached. This variation is caused by the form of the current distribution near an interface and in multiple scattering resonances between an interface and the impurity. An approach was formulated to treat mesoscopic systems, allowing the determination of the electromigration driving force and the associated microscopic electric (Continued on Reverse)

20. DISTRIBUTION/AVAILABILITY OF ABSTRACT ☒ UNCLASSIFIED/UNLIMITED ☐ SAME AS RPT ☐ DTIC USERS	21. ABSTRACT SECURITY CLASSIFICATION UNCLASSIFIED	
22a. NAME OF RESPONSIBLE INDIVIDUAL Mark W. Levi	22b. TELEPHONE *(Include Area Code)* (315) 330-2075	22c. OFFICE SYMBOL RADC (RBRP)

DD Form 1473, JUN 86   *Previous editions are obsolete.*   SECURITY CLASSIFICATION OF THIS PAGE

UNCLASSIFIED

Item 19 Continued:

field due to transport. Detailed analyses were prepared for the following mesoscopic
systems: one-dimensional disordered conductors; an impurity-layer or grain boundary sand-
wiched between reservoirs; and an impurity in the vicinity of a point contact (including
the case of conductance quantization). The connection between the local transport field
(LTF) and electromigration driving force has been explored, and the possibility of using
a scanning tunneling microscope (STM) to measure the LTF has been investigated. The STM
gives a qualitative measure of the LTF, and the latter is a measure of one component of
the electromigration driving force on an impurity. The effect of a thermal gradient on
atomic migration was investigated within a strong-coupling theory based on linear response
formalism. The resulting driving for thermomigration was found to be expressible in terms
of a heat of transport consisting of a ballistic component and a previously unknown temper-
ature-independent component which is related to the direct force in electromigration, and
which may be substantial in those systems where the direct-force valence differs appreci-
ably from the nominal valence.

EVALUATION
Contract Number F30602-85-C-0071
Electromigration in Metallic Microstructures

This effort has produced a most significant advance in the theory of electromigration and thermomigration. It has clarified the gap between the empirical methods used in avoiding the effects in practical usage and what a sound fundamental understanding would require. It is clear from this work that empirical methods are not going to be adequate for very long; actual geometries in integrated circuits are rapidly encroaching on the mesoscopic regime. Even at present IC geometries there are structures such as grain boundaries and small grain configurations for which the quantum mechanical effects should not be ignored.

MARK W. LEVI
Reliability Physics Section
Microelectronics Reliability Branch

TABLE OF CONTENTS

ABSTRACT

Theoretical studies of electromigration in metallic microstructures have been performed in the areas of atomic dynamics and electronic aspects of driving forces. A general formulation of electrical conductivity and electromigration in bulk systems, thin films, and other low-dimensional systems has been constructed. We have found that electromigration driving forces can be calculated from consideration of elastic scattering, although it is the inelastic part of the electron scattering that propels the migrating atom. However, non-adiabatic recoil effects were found to play an important role in the atomic migration of light interstitials at lower temperatures. Model calculations for electromigration at grain boundaries, dislocations and surfaces show substantial variation in driving forces as an interface is approached. This variation is caused by the form of the current distribution near an interface and in multiple scattering resonances between an interface and the impurity. An approach was formulated to treat mesoscopic systems, allowing the determination of the electromigration driving force and the associated microscopic electric field due to transport. Detailed analyses were prepared for the following mesoscopic systems: one-dimensional disordered conductors; an impurity-layer or grain boundary sandwiched between reservoirs; and an impurity in the vicinity of a point contact (including the case of conductance quantization). The connection between the local transport field (LTF) and electromigration driving force has been explored, and the possibility of using a scanning tunneling microscope (STM) to measure the LTF has been investigated. We found that the STM gives a qualitative measure of the LTF, and that the latter is a measure of one component of the electromigration driving force on an impurity. The effect of a thermal gradient on atomic migration was investigated within a strong-coupling theory based on linear response formalism. The resulting driving for thermomigration was found to be expressible in terms of a heat of transport consisting of a ballistic component and a previously unknown temperature-independent component which is related to the direct force in electromigration, and which may be substantial in those systems where the direct-force valence differs appreciably from the nominal valence.

2

I. INTRODUCTION

The main objective of our research program was to obtain a better theoretical description of electromigration in metallic microstructures. The major question we have addressed is "how is electromigration in a small metallic system affected by surfaces, interfaces and extended defects such as grain boundaries, atomic clusters and dislocations?" In answering this question, we have developed insights that will lead to a better understanding of the electromigration failure mechanism in VLSI circuits.

To guide future work in VLSI, it is important to have a better understanding of the physics of the electromigration process. At temperatures of device operation, the dominant driving force for electromigration is due to the momentum transfer to the atoms by the electrons that are flowing through the metal. This is the so-called electron wind force.[1] It follows that a better understanding of electromigration in metallic microstructures requires a better picture of the microscopic electronic current flow in metallic microstructures and a better picture of the dynamical response of atoms to the momentum transfer from the electronic system.

The notion of a microscopic driving force for electromigration is a subtle one, and despite its widespread use in virtually all theoretical work, it has not up-to-now been adequately justified. In Section II we investigate the nature of the driving force and show that for light impurity atoms there can be unexpectedly significant corrections arising from recoil effects that are not included in the standard Born-Oppenheimer adiabatic picture.

The electromigration driving force is ultimately connected to the local electric field accompanying the electron transport process. This local transport field is in fact the field which exerts the force on an impurity, as we illustrate in Section III. The transport field of interest is the electrostatic field arising from scattered electrons and from the long-range macroscopic field. A local field method is described which allows calculation of the microscopic electric field in the presence of current flow, and the results of explicit calculations are given in Section IV. Among the systems considered are grain boundaries, dislocations, thin films, one-dimensional disordered systems, point contacts and narrow constrictions. The feasibility of explicitly measuring the local transport field with a scanning tunneling microscope is also theoretically considered.

The problem of thermal gradients is briefly considered in Section V, where the result of a linear-response theory calculation for thermomigration is described. The calculations are based on a strong-coupling formalism which allows for arbitrarily strong scattering by impurities. As a result we find that an analogue of the direct force contribution in electromigration also arises in thermomigration.

II. DRIVING FORCE FOR ELECTROMIGRATION

In this section we examine the standard picture of the driving force for electromigration[1] and show that there may be significant corrections to this picture due to atomic recoil effects. The standard picture is based upon the Born-Oppenheimer approximation, which we now briefly outline.

A. Born-Oppenheimer Approximation

In the analysis of atomic diffusion in solids it is customary to picture the diffusing atom, or ion, as located in some static effective potential field obtained by calculating the total energy of the solid as a function of the position of the atom of interest. The effective field thus obtained includes contributions to the total energy of the solid from the energy of interaction of all the nuclei and electrons which are present in the crystal, and also the contributions from the kinetic energy of the electrons. The actual diffusion "jump" is then pictured as a thermally activated process in which the atom absorbs energy from its environment to surmount a local potential barrier separating its initial and final sites.

The existence of an effective force field governing the dynamics of the atoms in a solid finds its justification in the Born-Oppenheimer adiabatic approximation - the guiding principle being that since the ions are so much heavier than the electrons, the atoms move much more slowly than the electrons, which thus have enough time to re-adjust themselves to lower the total crystal energy at each point on the atom's path. One can then determine the effective field by observing how the total crystal energy changes as a function of the atom's position along a jump path in the solid. Within the Born-Oppenheimer approximation we thus determine a force field obtained by assuming that the atoms are fixed in position (or alternatively, act as if they were infinitely massive as far as their interactions with the electron gas is concerned), while the electrons are assumed to obey the Schroedinger wave equation. The force field obtained for the atoms can then

4

later be used in the Schroedinger wave equation for atomic motion, although for diffusion we usually need only consider classical atomic motion.

When electron currents are present it is clear that the dynamics of the electrons in the solid will be altered, and so too, the effective force fields. The force arising from the electron current and the attendant electron scattering is calculated within the Born-Oppenheimer approximation by assuming that the atoms are fixed in position, just as in the calculation of the force-field in the absence of current. Assuming that the atom of interest has bare valence Z and is at position $\vec{r}_o$, the bare potential seen by an electron at position $\vec{r}$ due to that ion is $V_b(\vec{r}-\vec{r}_o) = -Ze^2/|\vec{r}-\vec{r}_o|$, where e is the magnitude of the electron charge. It follows that the net force exerted on the ion due to the combined action of the non-equilibrium electron current or electron wind, and the macroscopic electric field $\vec{E}_o$ has the Feynman-Hellmann form[2]

$$\vec{F} = Ze\vec{E}_o - \int \delta n(\vec{r}) \frac{\partial V_b}{\partial \vec{r}_o} d^3r \qquad (1)$$

where $\delta n(\vec{r})$ is that part of the local electron density which is out of equilibrium, i.e., the part which depends on the electron current and the related transport field.

Now, within this picture, the force field $\vec{F} = \vec{F}(\vec{r}_o)$ lowers the barrier for diffusion preferentially in one direction, and this gives rise to a net atomic current. The appropriate effective force for the resulting electromigration is actually the average of $\vec{F}(\vec{r}_o)$ over the jump path, i.e.,

$$F_{eff} = \frac{1}{\ell_{AB}} \int_{\vec{r}_A}^{\vec{r}_B} \vec{F}(\vec{r}_o) \cdot d\vec{r}_o \qquad (2)$$

where $\vec{r}_A$ and $\vec{r}_B$ are the initial and final points in the jump path, and $\ell_{AB} = |\vec{r}_A - \vec{r}_B|$ is the jump distance. F_{eff} is the driving force for electromigration, and corresponds to an equivalent constant force that would lead to the same lowering of the energy between $\vec{r}_A$ and $\vec{r}_B$ as does the true force $\vec{F}(\vec{r}_o)$. That is, by construction, the energy is lowered by an amount $\Delta U = F_{eff}\ell_{AB}$ between sites A and B, which is exactly the same result as would be obtained by assuming a constant force field F_{eff} acting everywhere between A and B. The atomic current, J_a, is related to the effective force through the usual Nernst-Einstein relation, which in its simplest form is[1]

5

$$J_a - (DN_a/k_B T)F_{eff} \tag{3}$$

where D is the diffusion coefficient, N_a is the concentration of mobile atoms (or impurities) and $k_B T$ is the thermal energy at temperature T. Eq. (3) is valid for interstitial or vacancy diffusion mechanisms.

B. Recoil Effects

Now let us examine the validity of our previous assumption which regards the driving force for the electromigration as arising from a steady force $\vec{F}(\vec{r}_o)$. The major contribution to $\vec{F}(\vec{r}_o)$ usually arises from the electron-wind contribution contained in the second-term on the RHS of Eq. (1). Now, focussing on the electron-wind force, the assumption implicit in the Born-Oppenheimer adiabatic approach is that the electron-wind force is a steady (time independent) force. But the wind-force arises from the momentum transfer per second from the electrons to the atom during the scattering process, and this is not independent of time except in some long-time-average sense.

We expect that the adiabatic picture of a time-independent force is valid if the momentum transfer per collision, $\vec{p}_o$, is very small compared to the momentum of the atom, and if the rate of collisions, ν_{coll}, is moderately high so that a steady wind-force is meaningful. In the case of electromigration, however, these conditions are not met. For a metal, p_o is on the order of the Fermi momentum, and this is not necessarily small compared to the momentum of the atom. Also, collisions are rare events, i.e., even for high electron currents we have $\nu_{coll} \ll \nu_o$, where ν_o is the oscillation frequency of the impurity atom in its well.[3] We also note that the duration of a collision is very short on all time scales of interest, being on the order of r_o/v_F where r_o is the range of the potential and v_F is the Fermi velocity.[3] We are thus led to a model in which the atom is subjected to a random train of impulses, the time-dependent force being

$$\vec{F}(t) = \vec{p}_o \sum_n \delta(t-t_n) \tag{4}$$

where t_n are the random times of impact, and for simplicity, we have ignored any position-dependent variation in the rate of momentum transfer. We restrict attention to the regime of a low-intensity beam (small ν_{coll}) which is appropriate in the ohmic regime for transport since ν_{coll} is proportional to the electron current. A very dilute impurity-concentration is also

6

assumed. To allow for different directions of momentum transfer we can average our final results over all directions of $\vec{p}_o$ in the incident electron distribution.

Let us first investigate the case that p_o is arbitrarily small. The ensemble average velocity of an impurity atom can then be calculated from linear response theory,[4] with $H'(t) = -\vec{r}_o \cdot \vec{F}(t)$ being the perturbed hamiltonian for an impurity at $\vec{r}_o$. To first order in H' the i-th component of the average velocity is given by

$$\langle v_i(t) \rangle = \sum_j \int_0^\infty R_{ij}(t')F_j(t-t')dt' \tag{5}$$

where $R_{ij}(t') = i\hbar^{-1} \langle [v_i(t'),x_j] \rangle_{eq}$ is the standard Kubo correlation function for the equilibrium system.[4]

The physically relevant quantity is the time-average velocity over a long time T, i.e.,

$$\bar{v}_i = \lim_{T\to\infty} \frac{1}{T} \int_{-\frac{T}{2}}^{\frac{T}{2}} dt \langle v_i(t) \rangle . \tag{6}$$

From Eqs. (5) and (6) we have

$$\bar{v}_i = \sum_j \int R_{ij}(t')\bar{F}_j \, dt' \tag{7}$$

where

$$\bar{F}_j = \lim_{T\to\infty} \frac{1}{T} \int_{-\frac{T}{2}}^{\frac{T}{2}} F_j(t'')dt'' .$$

$$= \nu_{coll} P_{oj} . \tag{8}$$

We have thus established the result that to first-order in p_o the time average response to the impulse train $\vec{F}(t)$ is equivalent to the response to the time average force $\vec{F} = \nu_{coll}\vec{p}_o$, just as would be expected in the adiabatic picture.

Corrections to the adiabatic picture arise because the momentum transfer $\vec{p}_o$ is large enough for atomic-recoil effects to influence the atomic dynamics, thereby preventing the replacement of $\vec{F}(t)$ by $\vec{F}$. The effect of atomic recoil depends on the details of the atomic diffusion process. Here

we investigate the case of interstitial–impurity diffusion in the classical regime.

Consider an interstitial impurity atom in a harmonic potential energy well. In this highly idealized diffusion model the atom is assumed to complete a jump to a neighboring site when thermal fluctuations cause the atom to undergo an excursion beyond some critical displacement, $a_c \sim a/2$, where a is the distance between interstitial sites. In the absence of collisions with the electron current, the probability of the atom making a successful jump is $\exp(-\beta E^*)$ per attempt,[5] where E^* is the activation energy and $\beta = (k_B T)^{-1}$. The number of attempts per second is ν_o, which is the oscillation frequency of the atom in the well. The energy transfer in an electron–atom collision is typically much smaller than E^*, which implies that the collisions only affect the success rate for jumps that would have been very nearly successful in the absence of the electron current. For these jumps let the average velocity of the impurity be denoted by v_i^*. The corresponding atomic recoil energy in a collision is

$$\Delta E_R = \frac{1}{2M} [|\vec{p}_i^* + \vec{p}_o|^2 - |\vec{p}_i^*|^2] \tag{9}$$

where $\vec{p}_i^* = M\vec{v}_i^*$, and M is the mass of the atom. Note that in any given collision, it is the full recoil–momentum $\vec{p}_o$ which is transmitted and not the long–time–average momentum transfer, which is on the order of $\vec{p}_o \nu_{coll}/\nu_o$ and hence arbitrarily small as $\nu_{coll} \to 0$.

Now, only the part of ΔE_R which is odd in $\vec{p}_o$ can lead to a net atomic current. This allows us to ignore the p_o^2-term in Eq. (9). It then follows that a collision lowers the energy barrier E^* by an amount $\Delta E = v_i^* p_o \cos\theta$ where we have chosen the jump path to lie along the +x axis, and $\cos\theta = \hat{p}_o \cdot \hat{x}$. Similarly for diffusion jumps along -x, the barrier is raised by ΔE. Using the new activation energy for the fraction of jumps that experience a collision, we find an enhancement factor, Γ, given by

$$\Gamma \equiv \frac{J}{J_{ad}} = \frac{\langle \sinh \beta \Delta E \rangle}{\langle \beta \Delta E \rangle} \tag{10}$$

where J is the true atomic current including recoil effects, J_{ad} is the current in the adiabatic approximation, and $\langle ... \rangle = \int_0^1 d\cos\theta \cos\theta ...$, which arises from averaging over all angles of $\vec{p}_o$ in the out-of-equilibrium part of the shifted-Fermi-sphere distribution for incident electrons in a free electron model. We have taken the net electron particle-current to be along

8

the +x direction. In obtaining (10) we have used the result contained in Eq. (7), namely that J approaches J_{ad} in the $p_o \to 0$ limit. Evaluation of Eq. (10) yields $\Gamma = 3u^{-2}[\cosh u - u^{-1} \sinh u]$, where $u = \beta v_i^* p_o$.

Since v_i^* is larger for smaller M, Eq. (10) implies that, all other things being equal, a light impurity feels a greater driving force than a heavy one. This affords a possible explanation of the Häffner effect,[1] which is the observation that in an isotopic mixture of pure liquid-metals, it is the lighter isotope that invariably moves in the direction of the electron particle-current.

According to Eq. (10), the enhancement is small unless $\beta v_i^* p_o \gtrsim 1$. As an estimate we use $v_i^* \approx \nu_o a$, which is a typical velocity during a successful jump in the weak-damping regime, which is implicitly assumed in our analysis. As representative values for metals we take $p_o = 1$ a.u. $= 2 \times 10^{-19}$ g cm/s, $\nu_o = 6 \times 10^{-2}$ s^{-1}, and a = 2.6 Å. We then calculate that $\Gamma = 1.06$ at 300K and $\Gamma = 1.6$ at 100K. For light interstitials, Γ is expected to be larger due to the larger vibrational frequencies. As an example, for H in metals[6] ($\nu_o \gtrsim 2.5 \times 10^{13}$ s^{-1}) we find that $\Gamma \geq 2.4$ at 300K. However, for that system the diffusion process is considerably more complicated than our model allows, i.e., resonant modes, polaron-like distortions and quantum-mechanical diffusion processes should be considered.[6] The complexity of the H-diffusion process in metals may also account for the fact that our result yields a larger wind-force for hydrogen than for deuterium, but this is often not observed.[6] In any case, because Γ depends sensitively on v_i^*, and it is difficult to obtain a reliable estimate of v_i^*, our numerical estimates should be viewed with caution. For example, for the case $\nu_o = 6 \times 10^{12}$ s^{-1}, doubling our estimate of v_i^* gives $\Gamma \approx 1.3$ instead of 1.06 at 300 K.

Our conclusion as far as recoil-effects are concerned is that we do not expect very large corrections to the adiabatic picture unless we are considering light interstitials at lower temperatures (below room temperature). However, we cannot rule out interesting recoil effects for heavier impurities if the collision frequency ν_{coll} turns out to be extremely high due to huge electron-current densities (J ~ 10^{12} A/cm^2), such as might occur at a point contact in a nanostructure constriction.[7] For larger ν_{coll} the possibility of multiple collisions during the jump process becomes more likely and a non-linear response may occur, i.e., atomic current varying quadratically in the electron current density, for example. Further details

concerning the recoil-enhancement effect in the linear regime have been given elsewhere for both classical and quantum-mechanical diffusion processes.[8]

III. ELECTROMIGRATION AND THE LOCAL TRANSPORT FIELD

The connection between the electromigration driving force and the local electric field follows from the gedanken experiment used to operationally define an electric field. To determine the local electric field $\vec{E}_L(\vec{r})$ at position $\vec{r}$ we imagine placing a test charge Q at $\vec{r}$ and imagine measuring the force $\vec{F}$ on the test charge. The local electric field at $\vec{r}$ is then given by

$$\vec{E}_L(\vec{r}) = \lim_{Q \to 0} (\vec{F}/Q) . \tag{11}$$

Combining this operational definition and Eq. (1) with Q = Ze, we find that

$$\vec{E}_L(\vec{r}) = \vec{E}_o(\vec{r}) + e\nabla \int \frac{\delta n(\vec{r}')}{|\vec{r}-\vec{r}'|} d^3r' \tag{12}$$

where $\nabla = \partial/\partial\vec{r}$ and we have introduced the dummy variable $\vec{r}'$ in the integrand in Eq. (1).

It follows from Eqs. (1) and (12) that the force on any impurity having bare valence Z, i.e., having core charge Ze, and placed at position $\vec{r}_o$, is given by

$$\vec{F} = Ze \, \vec{E}_L(\vec{r}_o) \tag{13}$$

for arbitrary values of Z. Alternatively we can express $\vec{F}$ in the more common form by introducing an effective valence Z^* and writing

$$\vec{F} = Z^*e \, \vec{E}_o(\vec{r}_o) . \tag{14}$$

Eqs. (13) and (14) provide the connection between the local field $\vec{E}_L$ and the effective valence Z^*, which is traditionally taken as the central quantity in specifying electromigration driving forces. The important part is that if we can determine the local transport field $\vec{E}_L(\vec{r})$ we can immediately obtain the driving force for electromigration. Of course, $\vec{E}_L(\vec{r})$ must be determined for the system in the presence of all impurities. Here and in the remainder of this report we are assuming the validity of the adiabatic Born-Oppenheimer approach described in Sec. II.A.

Since the determination of $\vec{F}$ or Z^* is essentially a problem in determining the local transport field (LTF), we have focussed attention on

10

the determination of LTF. The results have been described in detail in a series of papers,[9-14] which we recapitulate in the current report.

We call our basic approach to the LTF "the local field method". The method is based in part on Landauer's picture of electron conduction in the presence of localized scatterers[15,16] and in part on insights which we have developed from previous work on electromigration.[17-21] In particular, our approach differs from Landauer's in that we place greater emphasis on the details of the quantum mechanical scattering process. Such details can be of crucial importance for microstructures, especially when impurities are situated near surfaces.

The local-field method provides a tractable scheme for determining the microscopic potential, the electrical resistivity, and the electromigration driving force on an impurity in a microstructure.[11] We now proceed to outline the basic ideas behind the method.

According to Landauer,[15] the increase in resistivity due to an impurity is associated with a microscopic dipolar source of electric field and current. This dipolar source is called the residual resistivity dipole (RRD). The RRD is not only a useful concept for the formulation of electron transport in microstructures, but is also important for understanding the detailed nature of the local field. An effective RRD can also be defined when the scatterer or a group of scatterers is in the neighborhood of interfaces of a microstructure, provided that the size of the scatterer group is not larger than the background mean free path ℓ. To understand how the RRD field is set up due to the scatterers, we consider a scatterer group in the vicinity of interfaces of a microstructure. The center of this scatterer group is at location $\vec{r}_o$. When electrons are scattered by the scatterer group and arrive at another position, say $\vec{r}$, there is a local pile-up of charges and the local potential is adjusted so as to neutralize the excess space charges. The local potential shift is the RRD field. It is then clear that for $|\vec{r}-\vec{r}_o| < \ell$, the local potential depends on the quantum mechanical scattering by the group and interfaces. When $|\vec{r}-\vec{r}_o| > \ell$, the local potential depends also on the background scattering, which we assume is incoherent in nature. The calculation of the local electrostatic potential is then divided into two regimes, namely, the near-field regime (region close to the scatterer group) and the far-field regime (region far from the scatterer group). Solution of the problem in the near-field regime requires a full

quantum—mechanical scattering treatment. The far-field regime defines a Boltzmann—type transport problem. Since the electromigration force depends only on the local scattering environment, the electromigration driving force can be found from consideration of the near field regime. However, in general, the electron distribution that is incident upon the scattering group is required and this will generally depend on the electron dynamics in the far-field region. The detailed nature of the fields and currents in the far-field region has been considered elsewhere.[9,11]

We consider a metallic microstructure connected to two highly conducting leads, one to the left-hand side and the other to the right-hand side of the microstructure. The microstructure can be a thin film, thin wire or even a superlattice. The leads are connected to electron reservoirs which supply electrons to, and drain electrons from, the microstructure. For simplicity we assume that the leads are made of the same material as the microstructure (i.e., they have the same electron density and the same mean free path due to background scattering). The microstructure itself contains additional impurities.

For the present, consider the case of a microstructure containing only a single impurity cluster, or scatterer group, whose size is characterized by the length L_c where $L_c < \ell$. The electrons incident upon the scatterer group are described by a shifted Fermi distribution which is set up by the background scattering that occurs in the leads and in the region of the microstructure far from the scatterer group. Assuming a free-electron-like bulk material, the part of the incident distribution that is out of static equilibrium is

$$g_k = -\tau e \vec{v}_k \cdot \vec{E}_o \delta(\epsilon_k - E_F) \ , \tag{15}$$

where τ is the electronic relaxation time associated with background scattering processes, $\vec{E}_o$ is the uniform macroscopic electric field in the absence of the scatterer group, $\vec{v}_k = \hbar \vec{k}/m$ is the electron velocity, $\epsilon_k = \hbar^2 k^2/2m$ is the electron energy, E_F is the Fermi energy, and m is the electron mass. The net particle current arising from the distribution in Eq. (15) is given by $\vec{J}_o = -n_o e \tau \vec{E}_o/m$, where n_o is the average density of conduction electrons in the microstructure.

In the near-field region, the general method is the following: First, we calculate the scattered wave function $\psi_k^{(+)}(\vec{r})$ for each electron incident in the plane-wave state $\psi_k^o(\vec{r}) = \Omega^{-1/2} \exp(i\vec{k} \cdot \vec{r})$ within the microstructure ($\Omega =$

volume). Second, we compute the perturbed electron density, $\delta n_w(\vec{r})$, due to the electron current (or "electron wind"). It is given by[11,20]

$$\delta n_w(\vec{r}) = \sum_k g_k |\psi_k^{(+)}(\vec{r})|^2 . \qquad (16)$$

Third, we determine the corresponding self-consistent electrostatic potential $\delta\Phi(\vec{r})$ from the Thomas-Fermi screening relation[11,15,20]

$$\delta\Phi(\vec{r}) = - \frac{\delta n_w(\vec{r})}{e(dn/dE)} , \qquad (17)$$

where dn/dE is the electronic density of states at E_F in the desired region of space. We remark that the self-consistent electron density is not δn_w, but is $\delta n_w + \delta n_s$, where δn_s is the induced screening charge which attempts to locally neutralize δn_w. Although $\delta\Phi$ in Eq. (17) is expressed in terms of δn_w, it actually arises from δn_w and δn_s. The microscopic electric field, $\delta\vec{E}_L(\vec{r})$, which is associated with the electron wind is determined from the potential through the usual relation

$$\delta\vec{E}_L(\vec{r}) = -\nabla\delta\Phi(\vec{r}) . \qquad (18)$$

Linear response is assumed throughout, i.e., only the response linear in E_o is considered. The total microscopic field includes the wind contribution $\delta E_L(\vec{r})$ of Eq. (18) plus the so-called direct-field contribution to be considered later.

Finally, the electromigration driving force due to the electron wind can be expressed in the general form[12]

$$\vec{F}_w(\vec{r}_o) = -\int \delta n_w(\vec{r}) \frac{\partial V}{\partial \vec{r}_o} d^3r \qquad (19a)$$

$$= - \sum_k g_k \langle\psi_k^{(+)}| \frac{\partial V}{\partial \vec{r}_o} |\psi_k^{(+)}\rangle \qquad (19b)$$

where $V = V(\vec{r}-\vec{r}_o)$ is the screened electron-impurity interaction, i.e., the final self-consistent potential after screening of the bare interaction $V_b(\vec{r}-\vec{r}_o)$ by the electron gas. It can be explicitly verified that for a single impurity in an electron gas, expression (19) is equivalent to the momentum-transfer expression[12]

$$\vec{F}_w(\vec{r}_o) = \sum_{kk'} \hbar(\vec{k}-\vec{k}')P_{kk'} g_k , \qquad (20)$$

where $P_{kk'}$ is the transitional probability for an electron being scattered (elastically) from state $\vec{k}$ to state $\vec{k}'$ by the impurity.

In general the net driving force on an impurity of pure valence Z at position $\vec{r}_o$ consists of the wind force plus the direct force, i.e.,

$$\vec{F}(\vec{r}_o) = \vec{F}_w(\vec{r}_o) + \vec{F}_d(\vec{r}_o) \tag{21}$$

where the direct force has the form[12]

$$\vec{F}_d(\vec{r}_o) = Ze\vec{E}_o(\vec{r}_o) - \int \delta n_d(\vec{r}) \frac{\partial V}{\partial \vec{r}_o} d^3r . \tag{22}$$

Here $\delta n_d(\vec{r})$ is the unscreened electron-density perturbation associated with the polarization due to the direct electrostatic field acting on the impurity. The local microscopic field $\vec{E}_L(\vec{r})$ thus consists of the wind contribution (18) plus a direct-field contribution equal to $\vec{E}_o(\vec{r})$ plus the contribution from the local polarization due to $\vec{E}_o(\vec{r})$.

Now, the direct force can be expressed as

$$\vec{F}_d(\vec{r}_o) = Z_d e\vec{E}_o(\vec{r}_o) \tag{23}$$

where Z_d is the effective valence associated with the direct field. We shall regard Z_d as a known quantity; it has been considered previously in a strong-coupling theory by Rimbey and Sorbello.[21,22] We concentrate instead on the wind force contribution in the present report. In any case, for nearly-free-electron-like metals, F_d is typically of order $(k_F \ell)^{-1}$ times F_w, and hence the direct force is relatively small compared to the wind force ($k_F \ell \gg 1$ even at high temperatures).

The key expressions of the local-field method are Eqs. (16)-(19). The specific form (15) for the incident electron distribution is appropriate for a free-electron gas in the presence of uniform background scattering. For the applications to be discussed in the next section, however, the specific form of g_k may differ from expression (15), but Eqs. (16)-(19) remain valid.

IV. APPLICATIONS

We now consider applications of the local-field method to bulk-like systems and mesoscopic systems. We define bulk-like systems to be those systems for which the system length, L, along the transport direction is much larger than the mean free path, ℓ, due to uniform incoherent (or inelastic) background-scattering processes. In the case of bulk-like systems the

14

incident electron distribution is taken to be set up by the uniform background-scattering. Thus, the localized scatterers are assumed to be relatively few and far between. In that case g_k has the form given in Eq. (15). Using this explicit form it is a relatively straightforward matter to calculate local fields and forces for various scattering complexes using Eqs. (16)-(19).

For the case of mesoscopic systems, which we define by the condition $L \ll \ell$, the incident distribution is specified in terms of a source and sink of electrons at the ends of the sample. More conveniently, we adopt Landauer's reservoir configuration,[23] in which ideal reservoirs are connected to each end of the sample.

We now describe calculations for the bulk-like systems including an impurity near a grain boundary, near a dislocation, and in an ultra-thin film. This is followed by a description of calculations for mesoscopic systems including a 1-d disordered conductor, a grain-boundary in the presence of an STM probe, and a point contact having an impurity in its vicinity.

A. Bulk-like Systems

Our calculations for bulk-like systems are based on the jellium model, with incoherent uniform background-scattering giving rise to the incident electron distribution g_k of Eq. (15). Before presenting the results for particular scattering complexes, we present a general relation between the net wind-force $\vec{F}_w$ on the scattering complex and the extra resistivity $\overset{\leftrightarrow}{\delta\rho}$ due to that complex. The desired relation is[12]

$$\vec{F}_w = - \frac{n_o e \Omega \overset{\leftrightarrow}{\delta\rho} \cdot \vec{E}_o}{\rho_o} \tag{24}$$

where ρ_o is the resistivity in the absence of the scattering complex. In general, the extra resistivity due to the scattering complex is a tensor, as implied by the notation $\overset{\leftrightarrow}{\delta\rho}$, because the complex may not be a spherically symmetric scatterer. In the case of spherically symmetric scatterers $\overset{\leftrightarrow}{\delta\rho} \cdot \vec{E}_o = \delta\rho \vec{E}_o$ in Eq. (24), where $\delta\rho = m/n_o e^2 \tau_{imp}$ and τ_{imp} is the usual momentum-weighted impurity relaxation time, i.e.,

$$\frac{1}{\tau_{imp}} = \sum_{k'} [1-\cos(\vec{k},\vec{k}')] P_{kk'} . \tag{25}$$

To derive Eq. (24) one makes use of Eq. (20), regarding the scattering complex as a single impurity for the purposes of the derivation.

In the bulk-like systems to be considered here the geometry will be such that the wind force of interest will be parallel to $\vec{E}_o$. It then follows from Eq. (24) that for this component (say along the x-direction)

$$F_w = -n_o e\Omega\delta\rho \; J_o \; , \tag{26}$$

where $\delta\rho$ refers to the diagonal element of the resistivity tensor $(\overset{\leftrightarrow}{\delta\rho})_{xx}$ and where $\vec{J}_o = \vec{E}_o/\rho_o$ is the electron current density in the absence of the scattering complex. The important point we wish to emphasize is that

$$F_w \propto \delta\rho \; J_{eln} \; , \tag{27}$$

where J_{eln} is the incident electron particle-current density. Eq. (27) states that the net momentum transfer per second to the scattering complex, i.e., F_w, is proportional to the extra resistivity (or residual resistivity) due to the scattering complex. Furthermore, for the examples to follow, the total momentum transfer (along the x-direction) to the scattering complex goes entirely to the single impurity in question which is in the vicinity of the extended structural defect, whether it be a grain boundary, dislocation or surface. The reason for this total momentum transfer going to the impurity is that the extended defects will be oriented to lie parallel to $\vec{J}_{eln}$, and since they will be modelled to have smooth (specular) interfaces, they will not absorb any momentum parallel to the interface.

We now present model calculations for an impurity in the vicinity of a grain-boundary, dislocation, and a surface of a thin film.

1. Impurity Near a Grain Boundary

In the jellium model a grain boundary can be modelled as a repulsive barrier,[24] which we take to be of height U and width d. This model ignores the details of the lattice mismatch at the boundary, and it replaces the effect of loose mis-fit at the grain-boundary as a region of lower density background positive charge, and therefore, a less attractive potential. This is equivalent to assuming a more repulsive potential in the grain boundary region compared to the uniform background potential. Choosing the z-direction perpendicular to the grain boundary, the model potential for the grain-boundary is taken to be

$$U(\vec{r}) = U_o \qquad 0 < z < d$$

$$= 0 \qquad \text{otherwise} \qquad (28)$$

where U_o is a constant. For simplicity we take the impurity to be a short-range isotropic scatterer which is modelled as a delta function potential given by

$$V(\vec{r}) = -v_o \delta(\vec{r}-\vec{r}_o) \qquad (29)$$

where v_o is a constant and the impurity is located at $\vec{r}_o$.

The wind force is calculated from Eqs. (16) and (19). To proceed it is necessary to obtain the scattering states $\psi_k^{(+)}(\vec{r})$. We regard the impurity potential strength v_o as a weak parameter, as indeed is consistent with the notion of modelling a physical potential by a delta function potential. The force on the impurity is desired to lowest order in v_o, i.e., to order v_o^2. Therefore we need to determine $\psi_k^{(+)}(\vec{r})$ to first order in v_o but to all orders in the grain boundary potential U_o. Using the results of scattering theory,[25] it is easy to show that up to terms linear in v_o the scattering states are given by

$$\psi_k^{(+)}(\vec{r}) = \phi_k^{(+)}(\vec{r}) + \sum_{k'} \phi_{k'}^{(+)}(r) \frac{<\phi_{k'}^{(+)}|V|\phi_k^{(+)}>}{E-E_{k'} + i\eta} \qquad (30)$$

where the $\phi_{k'}^{(+)}$ are the complete set of scattering states for the grain boundary potential U in the absence of the impurity, and the $E_{k'}$ are the corresponding energies of these states. The energy of the incident states is $E = E_F$, and η is a positive infinitesimal.

Now the wavefunctions $\phi_k^{(+)}(\vec{r})$ vary along the grain boundary interface as $\exp(i\vec{k}_{\parallel} \cdot \vec{r}_{\parallel})$ where $\vec{k}_{\parallel} = (k_x, k_y)$ and likewise $\vec{r}_{\parallel} = (x,y)$ since the unperturbed hamiltonian has translational invariance along the coordinates parallel to the interface. We take the incident electron current density $\vec{J}_{el}$ to lie parallel to the grain boundary, along the x-direction, say, and consider the x-component of the wind force on the impurity. From Eq. (19b) we have

$$(F_w)_x = -\sum_k g_k <\psi_k^{(+)}\left|\frac{[p_x,V]}{i\hbar}\right|\psi_k^{(+)}> \qquad (31)$$

where we used the fact that $\partial V/\partial r_o = -\partial V/\partial \vec{r} = [\vec{p},V]/i\hbar$, where $\vec{p}$ is the momentum operator. Now the matrix element of the commutator in Eq. (31) can

17

be simplified by noting that in the absence of the impurity there is translational invariance along the x-direction, and therefore the x-dependence of $\phi_k^{(+)}(\vec{r})$ enters through a factor $\exp(ik_x x)$. Combining this result and Eqs. (30) and (31) we find that

$$(F_w)_x - \frac{2\pi}{\hbar} \sum_{kk'} \hbar(k_x - k'_x) g_k |<\phi_k^{(+)}|V|\phi_{k'}^{(+)}>|^2 \delta(E_k - E_{k'}) \qquad (32)$$

which is of a form analogous to Eq. (20) if one adopts a golden-rule expression for $P_{kk'}$, replacing the incident plane wave states k,k' by $\phi_k^{(+)}, \phi_{k'}^{(+)}$, respectively.

The wavefunctions $\phi_k^{(+)}(\vec{r})$ are readily determined analytically from elementary considerations. Numerical calculation of the resulting expressions are straightforward, and involve only a double integral over angles on the Fermi surface. The results are shown in Figure 1 for the wind force $F_w(z)$ for an impurity at position z in the case of aluminum ($k_F = 0.9273$ a.u.) and assuming three different values of the ratio U_o/E_F, and taking the grain boundary width to be 5 a.u. $= 2.6\text{Å}$. Also shown in Figure 1 is the microscopic current density $j_x(z)$ which would exist at position z in the absence of the impurity. This local current density is determined from

$$j_x(z) - \text{Re} \sum_k g_k <\psi_k^{(+)}| \frac{P_x}{m} |\psi_k^{(+)}> \qquad (33)$$

where Re denotes the real part. Both $F_w(z)$ and $j_x(z)$ have been normalized to their bulk values so that far from the grain boundary they each approach unity. (The curves are then independent of the value of v_o.) Both $F_w(z)$ and $j_x(z)$ have even symmetry about the center of the grain boundary ($z - d/2$).

An interesting feature of Fig. 1 is that both the wind force and the local current density are substantially reduced within the grain boundary. A reasonable choice of barrier height, such as $U_o = 0.5 E_F$, leads to current and wind force values that are on the order of 30% of their bulk values when the impurity is within the grain boundary. It is also interesting that the wind force and the local current-density track somewhat closely, indicating that the wind force is qualitatively measuring the microscopic electron current. The wind force shows somewhat greater variations, however, both in terms of the overall reduction in the grain boundary region and in terms of the intensification of the Friedel oscillations outside the grain boundary.

18

The physical process behind the reduction of current and wind force at a grain boundary is that the region within the grain boundary is to some extent shielded from incident electrons. This occurs because incident electrons are reflected away at the z = 0 and z = d interfaces. In more pictorial language, we may say that the electron wind does not blow so hard within the grain boundary region.

There is an important implication that our calculations have on the 1/f-noise problem. According to standard theoretical models,[26] some recent 1/f-noise data can be explained if impurities hop between sites and if in the process their contributions to the resistivity change on the order of 20%. This size fluctuation is quite compatible with our results, which indicate that an impurity which hops inside a grain boundary will feel a relative reduction in wind force on the order of 10% to 50%. Such a relative change in wind force implies, by expression (27), an equivalent relative change in the resistivity contribution of the impurity in question. Thus our results do suggest that experimental data on 1/f-noise is compatible with the expected resistivity fluctuations for an impurity hopping near a grain boundary.

2. Impurity Near a Dislocation

We can perform an analysis for an impurity near a dislocation using methods similar to those which we employed for a grain boundary. Assuming a jellium model, we can model the dislocation core as a repulsive barrier in an otherwise uniform medium. The dislocation potential is modelled as

$$U(\vec{r}) = U_o \qquad 0 < R < a$$
$$= 0 \qquad R > a \tag{34}$$

where $\vec{r} = (\vec{R}, z)$ and $R = |\vec{R}|$ is the radial coordinate in cylindrical polar coordinate system. The axis of the dislocation core is along the z-axis and the incident current is also along the z-direction. The impurity is again modelled by the delta function form given in Eq. (29).

The derivation of the wind force follows the same lines as in the previous section for the grain boundary case. We deduce that the z-component of the wind force on the impurity is given by an expression precisely like Eq. (32) for $(F_w)_x$ except that the subscript x is replaced by z everywhere it appears in Eq. (32).

19

Again the wavefunctions $\phi_k^{(+)}(\vec{r})$ can be readily determined analytically from elementary considerations. In the usual way the wavefunctions are expressed as a sum of Bessel functions J_n and/or Hankel function H_n, with $\cos n\theta$ angular variation accompanying them. The expansion coefficients are determined by matching inner (R < a) solutions $J_n(k'R)$ and outer (R > a) solutions $J_n(kR)$ and $H_n(kR)$. The results are shown in Fig. 2a for the wind force $F_w(R)$ in the z-direction for an impurity located at a distance R from the dislocation axis. The metal is aluminum, and the dislocation radius is chosen to be a = 2 a.u. Also shown in Fig. 2b is the corresponding local current density $j_z(R)$ for the unperturbed problem, the latter being found from the right-hand side of Eq. (33) after the replacement of subscript x by z.

The qualitative features of the wind force and current curves are similar to those in Fig. 1 for the case of a grain boundary. Again we see large depletion of current and wind force in the barrier region.

3. Impurity in a Thin Film

We consider a thin film in the jellium model. The film surfaces are taken to be at z = ±d/2 and the impurity is taken to be at position z = d/2 - b, that is, at a distance b beneath the upper surface. The surfaces are assumed to be specular, resulting in a waveguide for electron waves. The incident electron wavefunction has the form

$$\psi_{n\vec{k}}^o = \sqrt{\frac{2}{\Omega}} \sin\left[\frac{n\pi}{d}(z + \frac{d}{2})\right] e^{i\vec{k}\cdot\vec{\rho}} , \qquad (35)$$

where $\vec{\rho} = (x,y)$, $\vec{k} = (k_x, k_y)$ and n is an integer which specifies the electron sub-band. The energy of the incident wave is the Fermi energy E_F, which results in different Fermi momenta k_{Fn} for the plane-wave portion of the wavefunction. Explicitly, $E_F = \hbar^2\left[k_{Fn}^2 + (\frac{n\pi}{d})^2\right]/2m$. For simplicity, we choose the impurity to be an isotropic scatterer of plane waves, which implies that it can be described in terms of an s-wave phase shift, δ_o. The scattering states $\psi_{n\vec{k}}^{(+)}(\vec{r})$ can be explicitly determined, and this has been given elsewhere.[11]

Calculations of the wind force and the resistivity change have been performed for several values of δ_o and these are shown as a function of d in Fig. 3 for the parameters appropriate to a film of CoSi$_2$, which has a bulk Fermi wavevector of 0.415 a.u. and an assumed mean free path ℓ = 200Å. The impurity is taken to be 2 a.u. from the surface (b ≈ 1.1Å). The curves show

the fractional change in film resistivity assuming a dilute concentration of impurities near the surface. The impurities are randomly located on the plane $z = d/2 - b$ and have concentration n_i impurities per unit area. The quantity $\Delta\rho/\rho_\infty$ is the net resistivity change $\Delta\rho$ divided by the resistivity ρ_∞ for an infinite bulk system. The connection between $(\Delta\rho/\rho_\infty)$ and the wind force is

$$F_{wind} \propto (\frac{\Delta\rho}{\rho_\infty})d\ J_o \ , \qquad (36)$$

which follows from Eq. (26). [The factor of d in Eq. (36) arises from the Ω-factor in Eq. (26).]

The results plotted in Fig. 3 reveal that significant quantum size effects occur for $d \leq 50$ a.u.. The jumps occur in the vicinity of new channels of waveguide propagation opening up as the distance d varies. This can also be described as due to the discontinuities in the electron density of states at a sub-band bottom. Parameters have been chosen so that for large d all curves approach the Fuchs–Sondheimer expression

$$\frac{\Delta\rho}{\rho_\infty} = \frac{3}{8}\ (1-p)\ \frac{\ell}{d} \qquad (37)$$

where p, the specularity parameter, was chosen to be 0.9. In general, our resistivity values tend to be higher than the Fuchs–Sondheimer expression (37).

We note that for larger values of δ_o (stronger scatterers) the curves dip-down where a new sub-band comes into play. This is especially evident for $\delta_o = 90°$. This lowering of the resistivity (and the wind force) can be traced to what we call a "transparency effect" which arises from multiple scattering between the impurity and the surfaces (or waveguide walls). In fact, if the background scattering were considerably weaker ($\ell \gtrsim 1000$ a.u.) the downward dips in Fig. 3 would extend virtually to zero in panels a, b and c. The Born approximation result is shown in panel d. Since the Born approximation is based on the weak scattering limit ($\delta_o \to 0$), the differences between the Born approximation curve and the others is indicative of the importance of multiple scattering between the impurity and the film surfaces.

B. Mesoscopic Systems

We now consider the local field and wind force in mesoscopic systems. The systems are assumed to be flanked by reservoirs on either side. These reservoirs act as a source and drain for electrons. Because the length of

the sample is assumed to be smaller than the background mean free path, these systems generally exhibit strong quantum mechanical interference effects.

1. One—dimensional Disordered Conductors

One—dimensional systems are interesting in their own right and have relevance for understanding quasi—one dimensional systems such as molecular chains or wires of extremely small cross section.

Consider a one—dimensional chain of potentials v_i representing a sequence of impurities in a one—dimensional system at zero temperature. The total potential has the form

$$V(z) = \sum_i v_i(z-z_i) \tag{38}$$

where z_i is the position of the i-th impurity. We shall take the impurity potentials to be localized and non—overlapping so that $V = 0$ regions exist between impurities.

We consider the Landauer configuration, where reservoirs acting as sources and sinks of electrons are attached to the ends of the chain. The length of the chain is L, and we assume that $L \ll \ell$, where ℓ is the mean free path for background scattering and other inelastic processes. We can therefore totally neglect all scattering processes other than the elastic electron—impurity scattering due to $V(x)$. This greatly simplifies the conductivity and electromigration problems.

Let the chemical potentials of the reservoirs be μ_1 and μ_2 on the left- and right-hand ends of the chain, respectively. Since we are concerned with linear response, we take $\Delta\mu = \mu_1-\mu_2$ to be arbitrarily small and positive. The reservoirs give rise to an incident distribution of electrons, g_k, where for each electron spin

$$g_k = \Delta\mu \; \Theta(k) \; \delta(\epsilon_k-\epsilon_F) \tag{39}$$

where $\Theta(k)$ is the unit step function, i.e., $\Theta(k) = 1$ for $k \geq 0$ and equals zero for $k < 0$. A positive (negative) value of k refers to electrons travelling to the right (left). The incident electrons in g_k are reflected or transmitted by the impurity chain, with probabilities R and T, respectively.

Calculation of the potential drop across the chain, using the one-dimensional forms of Eqs. (16) and (17) gives for the left- minus right-potential difference

22

$$\delta\Phi_L - \delta\Phi_R = -\frac{\Delta\mu R}{e} \qquad (40)$$

where we used the one-dimensional density of states $dn/dE = 2/\pi\hbar v_F$, including both spins. To obtain Eq. (40), we evaluated $\delta n_w(z)$ as an average of expression (16) over a window a few wavelengths in width. The effect of this is to eliminate cross-terms in $\delta n_w(z)$ due to the $\exp(\pm ikz)$ components of $\psi_k^{(+)}(z)$. This procedure is justified in the conductivity problem, where we are interested in a local average field, i.e., we want the persistent part of $\delta\Phi(\vec{r})$ and not the Friedel oscillations.

The net transmitted particle current, j_t, is given by

$$j_t = \frac{1}{L}\sum_k g_k v_k T = \frac{\Delta\mu}{\pi\hbar} T \qquad (41)$$

The resistivity, ρ, of the chain equals the average field divided by the charge current, i.e.,

$$\rho = \frac{-(\delta\Phi_L - \delta\Phi_R)/L}{-ej_t} \qquad (42)$$

which, after substitution of expressions (40) and (41), gives the celebrated Landauer formula[23]

$$\rho = \frac{\pi\hbar}{Le^2}\frac{R}{T} \qquad (43)$$

The Landauer formula is appropriate when the voltage probes measure the self-consistent potential $\delta\Phi(z)$ across the sample. In the experimental configurations thus far achieved, this is apparently not the case. Rather, it has been argued[27] that in a standard two-probe measurement between voltage pads, the relevant quantity is the chemical potential difference $\Delta\mu$ of the pads and not the electrostatic potential difference across the disordered region. In this case, the new resistivity, ρ', which includes the contact resistances at the conductor-reservoir interfaces, is given by[27]

$$\rho' = \frac{-(\Delta\mu/e)/L}{-ej_t} = \frac{\pi\hbar}{Le^2}\left(\frac{1}{T}\right) \qquad (44)$$

Now consider the electromigration force, F^i, on the i-th impurity in the chain, which we write as the sum of direct- and wind-forces, i.e., $F^i = F_d^i + F_w^i$. Since there is no background scattering, it follows that the external field $E_0(z_i)$ vanishes. Consequently, by Eq. (23),

$$F_d^i = 0 \qquad (45)$$

23

The vanishing of the direct force means that the impurity senses only the wind force. The latter is now evaluated from the momentum flux on the i-th impurity. Consider an electron incident onto the chain in state k, and let $a_L^+(k)$ and $a_L^-(k)$ be the plane wave amplitudes for the electron scattering state immediately to the left of the impurity. Specifically, a_L^+ and a_L^- are the coefficients of the exp(ikz) and exp(-ikz) components, respectively, of $\psi_k^{(+)}(z)$. Similarly, define $a_R^+(k)$ and $a_R^-(k)$ just to the right of the impurity. For a given incident k, the momentum/sec transferred to the impurity is found by calculating the product of the number of electrons/sec incident onto the impurity and the momentum carried per electron. The result is then summed over L,R, and +,-, taking into account direction of momentum flux. Finally a sum over k is performed. The result is

$$F_w^i = \sum_k g_k \, mv_k^2 \left[|a_L^+(k)|^2 + |a_L^-(k)|^2 - |a_R^+(k)|^2 - |a_R^-(k)|^2 \right] \qquad (46)$$

Expression (46) can also be obtained from Eq. (19), rather than by the present momentum-transfer analysis.

The wind force F_w^i bears no direct relationship to the additional resistivity due to the i-th impurity. However, the total force on the impurities is related to the total resistivity. To see this, use the global form of Eq. (46) for the entire system, in which case, the factor in parentheses in Eq. (46) equals 2R/L, and we obtain

$$F_w^{tot} = \frac{2k_F \Delta\mu R}{\pi} , \qquad (47)$$

where $F_w^{tot} = \sum_i F_w^i$.

Upon comparing Eqs. (40) and (47) we deduce that

$$F_w^{tot} = - \frac{2ek_F}{\pi} [\delta\Phi_L - \delta\Phi_R] . \qquad (48)$$

Thus, the total electromigration driving force directly measures the self-consistent potential drop across the conductor. We can re-cast Eq. (48) in terms of the Landauer resistivity (43). By inspection, we have

$$F_w^{tot} = -n_o eL\rho J_o \qquad (49)$$

where $n_o = 2k_F/\pi$ is the equilibrium 1-d carrier density and $J_o = -ej_t$ is the charge current. Note the striking similarity between Eq. (49) and the result (26) for a bulk system. In the case of a single impurity between reservoirs, F_w^{tot} is the wind force on the impurity, and ρ becomes the additional

24

resistivity due to that impurity. Then Eq. (29) becomes the 1-d form of Eq. (26), despite the fact that Eq. (26) refers to a bulk-like system dominated by background scattering.

We have performed explicit calculations of the wind force by means of Eq. (46). The amplitudes $a_L^{\pm}, a_R^{\pm}$ are easy to calculate by means of the transfer-matrix method.[28] For a series of randomly placed barriers in a one-dimensional line we calculated the electron scattering, electromigration driving forces (or local electric field) and overall resistivity of the configuration. We chose the impurity locations randomly for a given number N of impurities on a given size chain length, L. Nominally we chose N = 10 on a length of 100 equally spaced sites totalling 200 Å. We found very large variations among systems of the same N and L. Ensemble averages and statistical deviations were calculated for the average force on the impurities, the force on each impurity and the overall resistivity (determined from the Landauer formula). Changes in these quantities were also calculated when one impurity is moved over by one lattice site (simulating the effect of a diffusion jump) and also when one impurity is turned off, or destroyed. Our one-dimensional calculations indicate that the electromigration wind force varies dramatically over the impurities in the chain. The average force, therefore, may not be a true indication of the amount of electromigration damage, since the latter may nucleate from the weakest link in the chain. Furthermore, moving one impurity or destroying one impurity typically leads to a force distribution (among the remaining impurities) that is very different from the original force distribution. In fact, we found that the effect of moving a single impurity can be equivalent to choosing a totally scrambled configuration of impurities in the ensemble. The reason that the slight atomic re-arrangement associated with the motion of one impurity typically gives as drastic an effect as totally scrambling the positions of all atoms in the system is that the 1-d system is, in effect, a delicate interferometer for electron waves.[28]

We found that the particular distribution of electron density, local field and forces depends sensitively on the specific configuration of impurity scatterers. We calculated relevant quantities for an ensemble of identical impurities, each one described by a square-well potential of depth 0.5 a.u. and width one angstrom, which are typical values for metals. One thousand different impurity configurations were randomly generated. For this

25

ensemble we calculated histograms giving the number of systems having electromigration wind forces within certain ranges. Normalizing these results we obtain a probability distribution function, f, in histogram form. The distribution functions were calculated for the following quantities: the average wind force, $\overline{F}$, where the average is over the ten impurities in a given configuration; the wind force on the middle impurity (number five in the chain of ten), F_{mid}; and the Landauer resistivity, ρ, given by Eq. (43). The results are shown in Figure 4.

The wide extent of the distribution functions is remarkable. Note that although $\overline{F}$ is always negative, indicating a force in the direction of the electron wind, F_{mid} has significant probability of being positive, and can be quite large compared to the force for the single impurity system, the latter force being equal to -1.0 units for our chosen normalization. The resistivity distribution, shown in Fig. 4c, also has a substantial width. Note the large fluctuations and the increased presence of highly transparent systems (small R). Large fluctuations are a hallmark of small, low-dimensional systems, and one can also expect electromigration damage to vary considerably among such systems. The wide extent of the distributions calls into question the usefulness of simply reporting ensemble average values for forces, fields and resistivity.

A basic difficulty in trying to use 1-d systems as an indicator of behavior to be expected in bulk-like 3-d systems is that the response for 1-d systems is extremely sensitive to details concerning location and strength of the impurity scatterers. The disordered 1-d system is unique in this regard.[28] For this reason we did not push the 1-d calculations further.

2. Grain Boundary and an STM Probe

We have investigated the local field and wind force exerted on a planar grain boundary which is oriented perpendicular to the direction of transport in a mesoscopic system, again assuming the jellium model.[12] The voltage drop occurs in the immediate vicinity of the grain boundary,[12,16] but there is no explicit connection between the net wind force on the grain boundary structure and the resistivity due to the grain boundary.[12] That is, the analogue of Eq. (49) does not apply.

An interesting question concerns the possibility of measuring the potential drop across a grain boundary by means of the STM, as has recently been experimentally attempted.[28a] We investigated this possibility

26

theoretically[14] and found that across the grain boundary, the voltage drop measured by the STM, δV_{STM}, is of the same order of magnitude as the true voltage drop associated with the local transport field, δV_{LTF}. There are cases where the STM does measure δV_{LTF}, and these are the ultra-thin film case when only one sub-band is occupied and the case of a random distribution of parallel semi-classical barriers.[14] The fact that δV_{STM} and δV_{LTF} are of the same order of magnitude is a somewhat surprising result because according to Eq. (17), the LTF potential is proportional to the local pile-up of electron density associated with the electron scattering states, while the STM does not directly measure this electron pile-up. Rather, the STM is most sensitive to those electron wavefunctions that extend farthest outside the surface,[29] and these electron states are not necessarily representative of the total set of electron states involved in the LTF. Thus, we do not expect the STM voltage to measure the LTF. However, we find that the STM gives a qualitatively useful measure of the LTF. This is shown in Figure 5 where δV_{STM} and δV_{LTF} are plotted as a function of W, which is the thickness of the thin film which contains the grain boundary. The δV's are in units of the chemical-potential difference $\Delta \mu$ of the reservoirs, and W is in a.u.. We note the jumps corresponding to quantum size effects associated with density-of-states discontinuities at sub-band bottoms, as previously mentioned in regard to Fig. 3. We also point out that δV_{STM} exhibits larger quantum size effects than δV_{LTF}, and this suggests that the STM can be an effective probe of the quantum size effects.

3. Impurity Near a Point Contact

The flow of electrons through a point contact gives rise to strong variations in the local electric field and produces an associated contact resistance. We now address the point-contact problem in detail.

Consider the standard theoretical model of a point contact[30] as a circular aperture, of radius a, on an opaque plane, z = 0, which separates two halves of an electron gas. A negative potential difference $-\Phi_o$, is applied across the contact from the left-hand side (z<0) to the right-hand side (z>0). This raises the Fermi level of the electron gas on the left-hand side by an amount $\Delta \mu = e\Phi_o$ with respect to the Fermi level on the right hand side, thereby causing a net flow of electrons through the aperture, from left to right. The spreading of electrons as they emerge from the aperture gives rise to local variations in the electron density, current and potential.

27

The aperture acts as a bottleneck to electron flow, and gives rise to the so-called "spreading resistance" or Sharvin resistance for a point contact, namely,[30]

$$R_{Sharvin} = \frac{4\pi\hbar}{e^2 k_F^2 a^2} \qquad (50)$$

Eq. (50) holds in the regime where background scattering is negligible and the aperture diameter is substantially greater than an electron wavelength, so that wave-diffraction effects at the aperture can be neglected. For the present, we shall also restrict our analysis to this regime.

To apply the method of Sec. III, we need the electron distribution function. For definiteness, consider a point $\vec{r}$ in the $z > 0$ region. There is an excess distribution of electrons at this point, $g_{\vec{k}}(\vec{r})$, over and beyond the equilibrium distribution that would exist in the $z > 0$ region if no aperture were present. The excess is due to the additional electrons from the $z < 0$ region that can reach point $\vec{r}$ by propagating ballistically through the aperture. (Recall that we are in the regime where wave diffraction and background scattering are neglected.) Thus,

$$g_{\vec{k}}(\vec{r}) = \Delta\mu \; \delta(\epsilon_k - \epsilon_F) \quad \text{for} \quad \vec{k} \in \Omega_o(\vec{r}) \qquad (51)$$

where $\Omega_o(\vec{r})$ is the solid angle defined by the sheaf of all straight-line trajectories emerging from the point $\vec{r}$ after having come through the

aperture. (When $\vec{r}$ is on the axis of the aperture, $\Omega_o(\vec{r}) = 2\pi[1 - z/\sqrt{a^2 + z^2}]$.)

In possession of $g_{\vec{k}}(\vec{r})$ and $\psi_{\vec{k}}^{(o)} = \exp(i\vec{k}\cdot\vec{r})$, we can apply the machinery of Sec. III to determine local fields and forces on an impurity near the aperture. By keeping track of the flux of electrons through the aperture, it is straightforward to derive the Sharvin resistivity expression (50) in the absence of an impurity, and to derive the additional resistivity δR due to an impurity. The results have been presented elsewhere.[12] We found that the wind force can be expressed in terms of the local current density $\vec{J}(\vec{r}_o)$ at the position of the impurity. Specifically, the expression is[12]

$$\vec{F}_w(\vec{r}_o) = -\frac{m\Omega\vec{J}(\vec{r}_o)}{e \; \tau_{imp}} \qquad (52)$$

where τ_{imp} is the bulk impurity scattering time, and is given by Eq. (25). Expression (52) is a microscopic version of Eq. (24), and takes into account

that the current may vary substantially in the aperture region due to the bottleneck effect.

Equation (52) shows that the wind force scales with current density just as for the bulk system. When an impurity is very near the aperture, therefore, the actual current density at the aperture is the relevant quantity, and we can estimate the wind force as

$$F_w \cong K\left(\frac{I}{\pi a^2}\right) \tag{53}$$

where $K = F_w|_{bulk}/J_{bulk}$. The approximation (53) is excellent for an impurity in the aperture ($z=0$).

Because of the huge current densities that can be supported at a point contact, the wind-force can be several orders of magnitude greater than in the bulk case. For a small aperture, the direct force is even more greatly enhanced with respect to bulk values because the external electric field E_o at the aperture is on the order of $\Phi_o/2a$, since the potential drop essentially occurs within a distance $2a$.[12,30] To estimate the relative importance of these forces, we use Eqs. (23) and (53) and find

$$\frac{F_d}{F_w} \cong -\frac{Z_d e}{K}\left(\frac{2\pi^2\hbar}{e^3 k_F^2 a}\right) , \tag{54}$$

where we have used $\Phi_o = IR_{Sharvin}$ and expression (50). Note that, in principle, $|F_d| > F_w$ when a is sufficiently small (provided that $k_F a \gg 1$ so as not to contradict our neglect of diffraction at the aperture). Using $Z_d = Z$ and the calculated value of K for aluminum from Ref. 31, we find that Eq. (54) gives $F_d \cong -\frac{1}{2} F_w$ for self-electromigration in aluminum when $a \cong$ 14Å. This is in marked contrast to the case of bulk free-electron-like metals where

$$\frac{F_d}{F_w}\bigg|_{bulk} = -\frac{Z_d e \rho_o}{K} . \tag{55}$$

Evaluation of this expression using values appropriate to nearly-free-electron conductors yields $|F_d|$-values which are typically much smaller than F_w-values even at high temperature.

The relative enhancement of the direct force in the region of a point contact implies that point contacts may be useful as a probe of the most elusive and controversial aspect of electromigration theory, namely, the direct force.

Thus far we have considered point contacts of essentially zero width and have restricted attention to the semi-classical regime of larger aperture sizes, where quantum mechanical wave interference is negligible. Recently it has been discovered that narrow channels which serve as point contacts in a 2-d electron gas do not act in a semi-classical manner, but rather display the novel phenomenon of conductance quantization.[32] That is, the conductance, G, as a function of constriction width W takes on values G = $2ne^2/h$ where n is an integer. (W is continuously varied in these experiments by means of a gate voltage.)

We have studied the effect of disorder on the quantized conductance by considering an impurity present in the narrow channel of the point contact. Since the mean free path is greater than the dimensions of the narrow channel, weak disorder considerations are sufficient for the actual experimental situation. The narrow channel is modeled as an electron waveguide and the edge effect at the ends of the narrow channel is neglected. In using this model, we have implicitly assumed that the conductance of the narrow channel, before any disorder or impurity is introduced, has already well-developed plateau structures.

The present model for an impurity in a narrow channel is similar to our model in Sec. IV.C for an impurity in a thin film. In our previous study we considered the thin film to be a planar waveguide; in the present study we consider the narrow channel to be a waveguide of finite cross section. Previously, we found that the residual resistivity due to an impurity in a thin film exhibits interesting features due to the multiple-scattering of electrons between the impurity and the surfaces of the thin film. These features include resonance-like structures and a "transparency effect", which refers to a vanishing scattering cross section for the impurity. The transparency effect was found to occur when the film thickness is such that the Fermi level coincides with a sub-band minimum. Similar effects occur in narrow constrictions.

The result for a calculation of the conductance of a narrow, rectangular, 100Å thick channel is shown in Fig. 6. The dashed lines show the conductance in the absence of an impurity. The full curves show the conductance for an isotropic (s-wave) impurity with phase-shift δ_o = 30°. We have used typical experimental values of the 2-d Fermi wavelength ($\lambda_F \approx 500Å$)

and have taken the impurity to be at a distance of 50Å (in width) from the center of the channel.

The results show that the effect of an impurity is to lower the conductance and to round-off some of the plateau structure. We remark that the downward dips between neighboring plateaus are a consequence of multiple scattering between the impurity and the walls of the channel. This can be appreciated from the analytical expression that was derived for G and was presented elsewhere.[13]

As far as electromigration in the narrow channel is concerned, we expect from our previous studies that the wind force is essentially proportional to the additional resistivity due to the impurity. In that case, since $(\Delta G/G) \approx -(\Delta R/R)$, it follows that the wind force is proportional to the separation between the dashed and full curves in Fig. 6. In particular, at a sub-band bottom ($2W/\lambda_F$ = integer), where G remains pinned at the quantized value, there is no wind force because the impurity is effectively transparent at that point. At the downward dips between plateaus, however, the wind force is greatly enhanced due to multiple scattering effects.

V. THERMOMIGRATION

The effect of a temperature gradient on impurities in a solid can be treated by techniques similar to those employed for electromigration. The quantity analogous to the electromigration effective valence Z^* is the heat of transport, Q, for thermomigration. The driving force for thermomigration is expressed in the form

$$\vec{F} = -Q(\nabla T/T) \tag{56}$$

where ∇T is the macroscopic temperature gradient in the system. Eq. (56) is analogous to the expression $\vec{F} = -Z^* e \nabla \Phi_o$ for electromigration.

We have evaluated Q using Green's function techniques within the Kubo linear-response formalism, which we previously employed in the study of electromigration.[21] The calculations were performed within a jellium model, and the electron-impurity coupling was allowed to be arbitrarily strong. This strong-coupling theory[33] represents a significant advance upon previous thermomigration theories, which are based upon the weak-coupling approximation.[34]

The heat of transport can be schematically written in the following form as an expansion in inverse powers of $E_F\tau$:

31

$$Q = a(E_F\tau)^1 + b(E_F\tau)^0 + c(E_F\tau)^{-1} + \ldots \tag{57}$$

In the case of electromigration, one has the analogous expansion

$$Z^* = a'(E_F\tau)^1 + b'(E_F\tau)^0 + c'(E_F\tau)^{-1} + \ldots \tag{58}$$

Now since $E_F\tau = k_F\ell$ is typically much greater than unity we expect that the first term dominates the subsequent terms in Eqs. (57) and (58). In the electromigration problem we previously found that a' is the electron wind term and that b' is a consequence of the direct force. (Recall that the direct force is formally of order $(k_F\ell)^{-1}$ times the wind force.) The coefficients a',b' were related to on-energy-shell and off-energy-shell integrations over the T-matrix, respectively.[21] [There are additional contributions to b' which are properly considered to be vertex corrections to the on-energy-shell integrations, and these contributions makes it difficult to calculate the b'-term with accuracy.]

Previous calculations of Q succeeded in calculating only the leading term in Eq. (57) and this only for the case of weak scattering.[34] Our strong-coupling theory[33] reproduces that so-called ballistic-theory result, namely,

$$a(E_F\tau)^1 = -\frac{\pi^2}{3}(k_BT)^2 Z_w \left.\frac{d \ln[v(E)\sigma(E)]}{dE}\right|_{E=E_F} \tag{59}$$

where $Z_w = -n_o\tau v_F\sigma(E_F)$, with $\sigma(E)$ being the transport collision-cross-section at energy E. The quantity Z_w is the wind-force contribution to Z^*, i.e., the leading term in expansion (58).

We also calculated a new contribution, namely, the second term in expansion (57). This contribution can be written as[33]

$$b = \int_0^{E_F} [Z_d(E)-Z(E)]dE \tag{60}$$

where $Z_d(E)$ represents the electromigration direct-force valence corresponding to an electron gas having Fermi energy E, and Z(E) is the energy-dependent bare-valence, which is related to the impurity scattering phase shifts $\delta_\ell(E)$ by the usual Friedel sum-rule, namely, $Z(E) = (2/\pi)\sum_\ell(2\ell+1)\delta_\ell(E)$. We remark that the contribution (60) is not necessarily small compared to contribution (59) because the latter contains the factor $(k_BT)^2$, which is small at low temperature.

Our heat of transport contribution (60) arises entirely from the polarization of the electron gas by the impurity in the presence of a thermal gradient. It is associated with, but not equal to, the difference between the direct force and the bare valence in electromigration, since these are given by $Z_d(E_F)$ and $Z(E_F)$, respectively. We have performed model calculations of b using a Koster-Slater model similar to that which we used for the electromigration problem. We find that b-values on the order of tenths of E_F are possible.[33] Clearly, the contribution (60) is expected to be most appreciable in those cases where the direct-force valence and the bare valence are significantly different. It would be worthwhile to make careful measurements of both Z^* and Q in such systems and to look for the predicted correlations. We expect that Z_d and Z will differ the most for strong scatterers. Hydrogen in simple metals would be good systems for such studies.

VI. CONCLUSION

We have seen how a general theory of conduction and electromigration can be applied to a wide variety of systems. The approach requires knowledge of the incident electronic carrier distribution g_k. Given this distribution, all effects of quantum-mechanical multiple scattering are included in the formalism. We have also considered the role of non-adiabatic atomic recoil effects, and found them to be appreciable for light impurities at lower temperatures. A new contribution to the thermomigration driving force has been obtained, and it has been shown to be related to the direct force in electromigration.

Our investigations have revealed that there are large variations in the microscopic currents, the local electric field, the local resistivity, and the electromigration driving force near surfaces, interfaces, grain boundaries and dislocations. Calculations have been made for various models, and they show that marked variations arise from two features: First, the intrinsic variations due to extended defects, boundaries, interfaces in the absence of the impurity; and second, the multiple scattering effects (including resonances) between the intrinsic structure and the impurity undergoing electromigration. These effects are generally to be expected in all realistic modelling of electromigration driving forces in metallic microstructures.

REFERENCES

1. H. B. Huntington, in _Diffusion in Solids_, edited by A. S. Nowick and J. J. Burton (Academic, New York, 1975).
2. R. S. Sorbello and B. B. Dasgupta, Phys. Rev. B $\underline{21}$, 2196 (1981).
3. Typical numbers for metals: For an electron current density of 10^5 A/cm^2, collision cross section 1 Å^2, and $v_F = 2 \times 10^8$ cm/s, we have $\nu_{coll} \sim 10^8$ s^{-1}. Whereas, $\nu_0 \sim 10^{13}$ s^{-1}, and with $r_0 \sim 1$ Å, we have $r_0/v_F \sim 10^{-16}$ s.
4. R. Kubo, J. Phys. Soc. Japan $\underline{12}$, 570 (1957).
5. See, for example, L. A. Girifalco, _Statistical Physics of Materials_ (Wiley, New York, 1973).
6. H. Wipf, in _Hydrogen in Metals_, Vol. 2, edited by G. Alefeld and J. Völkl (Springer, New York, 1978), Chapter 7.
7. K. S. Ralls and R. A. Buhrman, Phys. Rev. Lett. $\underline{60}$, 2434 (1988).
8. R. S. Sorbello, "Recoil Enhanced Atomic Migration" (to be published).
9. R. S. Sorbello and C. S. Chu, IBM J. Res. Dev. $\underline{32}$, 58 (1988).
10. R. S. Sorbello and C. S. Chu, Superlattices and Microstructures $\underline{3}$, 467 (1987).
11. C. S. Chu and R. S. Sorbello, Phys. Rev. B $\underline{38}$, 7260 (1988).
12. R. S. Sorbello, Phys. Rev. B $\underline{39}$, 4984 (1989).
13. C. S. Chu and R. S. Sorbello, "Effect of Impurities on the quantized Conductance of Narrow Channels," Phys. Rev. B (in press).
14. C. S. Chu and R. S. Sorbello, "Scanning Tunneling Microscope as a Probe of the Local Transport Field," Phys. Rev. B (in press).
15. R. Landauer, IBM J. Res. Dev. $\underline{1}$, 223 (1957).
16. R. Landauer, Z. Phys. B $\underline{68}$, 217 (1987).
17. R. S. Sorbello and B. Dasgupta, Phys. Rev. B $\underline{16}$, 5193 (1977).
18. L. J. Sham, Phys. Rev. B $\underline{12}$, 3142 (1975).
19. W. L. Schaich, Phys. Rev. B $\underline{13}$, 3360 (1976).
20. R. S. Sorbello, Phys. Rev. B $\underline{23}$, 5119 (1981).
21. P. R. Rimbey and R. S. Sorbello, Phys. Rev. B $\underline{21}$, 2150 (1980).
22. R. S. Sorbello, Phys. Rev. B $\underline{31}$, 798 (1985).
23. R. Landauer, Philos. Mag. $\underline{21}$, 863 (1970).
24. A. Seeger, Can. J. Phys. $\underline{34}$, 1219 (1956); J. R. Smith and J. Ferrante, Phys. Rev.B $\underline{34}$, 2238 (1986).
25. B. Lippmann and J. Schwinger, Phys. Rev. $\underline{79}$, 469 (1950).
26. N. M. Zimmerman and W. W. Webb, Phys. Rev. Lett. $\underline{61}$, 889 (1988); J. Pelz and J. Clarke, Phys. Rev. B $\underline{36}$, 4479 (1987).
27. A. D. Stone and A. Szafer, IBM J. Res. Dev. $\underline{32}$, 384 (1988); R. Landauer, Ibid., $\underline{32}$, 306 (1988).
28. See, for example, M. Ya. Azbel, Phys. Rev. B $\underline{28}$, 4106 (1983), and references cited therein.
28a. J. R. Kirtley, S. Washburn and M. J. Brady, Phys. Rev. Lett. $\underline{60}$, 1546 (1988).
29. J. Tersoff and D. R. Hamman, Phys. Rev. Lett. $\underline{50}$, 1998 (1983).
30. I. O. Kulik et al., Sov. J. Low Temp. Phys. $\underline{3}$, 740 (1977).
31. R. S. Sorbello, J. Phys. Chem. Solids $\underline{34}$, 937 (1973).
32. B. J. van Wees et al., Phys. Rev. Lett. $\underline{60}$, 848 (1988).
33. P. R. Rimbey and R. S. Sorbello, Phys. Rev. B $\underline{38}$, 1095 (1988).
34. H. B. Huntington, J. Phys. Chem. Solids $\underline{29}$, 1641 (1968); M. Gerl, Z. Naturforsch. $\underline{26a}$, 1 (1971); W. Jones, J. Phys. F $\underline{12}$, 87 (1982).

FIGURE CAPTIONS

Figure 1 a) Electromigration wind force on an impurity at position z in the vicinity of a grain boundary in aluminum. The grain boundary is modelled by a barrier occupying the region d>z>0, where d = 5 a.u. Results are shown for the cases U_o/E_F = 0.1, 0.5, and 0.99, where U_o is the barrier height. The curves are individually normalized to their bulk values, i.e., they are made to approach unity far from the grain boundary.

b) Local current density parallel to the grain boundary in the absence of the impurity for the same U_o/E_F values of panel (a). The curves are normalized to their bulk values.

Figure 2 a) Electromigration wind force on an impurity at position R from the axis of a dislocation, which is modelled as a core consisting of a potential barrier of height U_o and radius a = 2 a.u. in aluminum. The curves shown are for the cases U_o/E_F = 0.1, 0.5 and 0.9. All quantities are normalized to bulk values.

b) Local current density parallel to the dislocation in the absence of the impurity for the same U_o/E_F values of panel (a). The curves are normalized to their bulk values.

Figure 3 Resistivity ($\Delta\rho/\rho_\infty$) due to impurities in a thin film is plotted as a function of $\log_{10}(d)$, where d is in a.u. The parameters are k_F = 0.415 a.u., ℓ = 200 Å, and (a) δ = 30°, n_i = 0.412×10^{-2} a.u.; (b) δ = 60°, n_i = 0.918×10^{-3} a.u.; (c) δ = 90°, n_i = 0.926×10^{-3} a.u. The Born approximation result is shown in (d). The number of occupied subbands from 1 to 7 is indicated above the abscissa. The impurity density values n_i were chosen to give the asymptotic Fuchs–Sondheimer result for p = 0.9. The latter is indicated by dot–dashed curves in (a), (b), and (c).

Figure 4 Distribution functions for ensemble of 1000 one-dimensional systems containing ten impurities. Electrons are incident at Fermi wavevector appropriate to bulk aluminum. The distributions are for the following:

a) average wind force in a system

b) wind force on the fifth impurity

c) resistivity of a system in units of $\pi\hbar/Le^2$.

The wind forces in a) and b) are divided by the magnitude of the corresponding wind force that would be exerted on a single impurity. A negative force indicates a force in the direction of the electron wind.

Figure 5   Voltage drops δV_{STM} and δV_{LTF} across a grain boundary in an aluminum film plotted as a function of W, the film thickness. The voltages are expressed in units of $\Delta\mu$, the chemical potential difference between the reservoirs. W is in atomic units (1 a.u. ≈ 0.53 Å).

Figure 6   Conductance G of an electron waveguide plotted as a function of the width, W, of the 100Å thick channel. The curve is for an attractive weak-scattering impurity with phase shift δ_o = 30°. The perfect waveguide result is indicated by the dashed steps. The difference between the dashed and full curves is a measure of the electromigration wind force on the impurity.
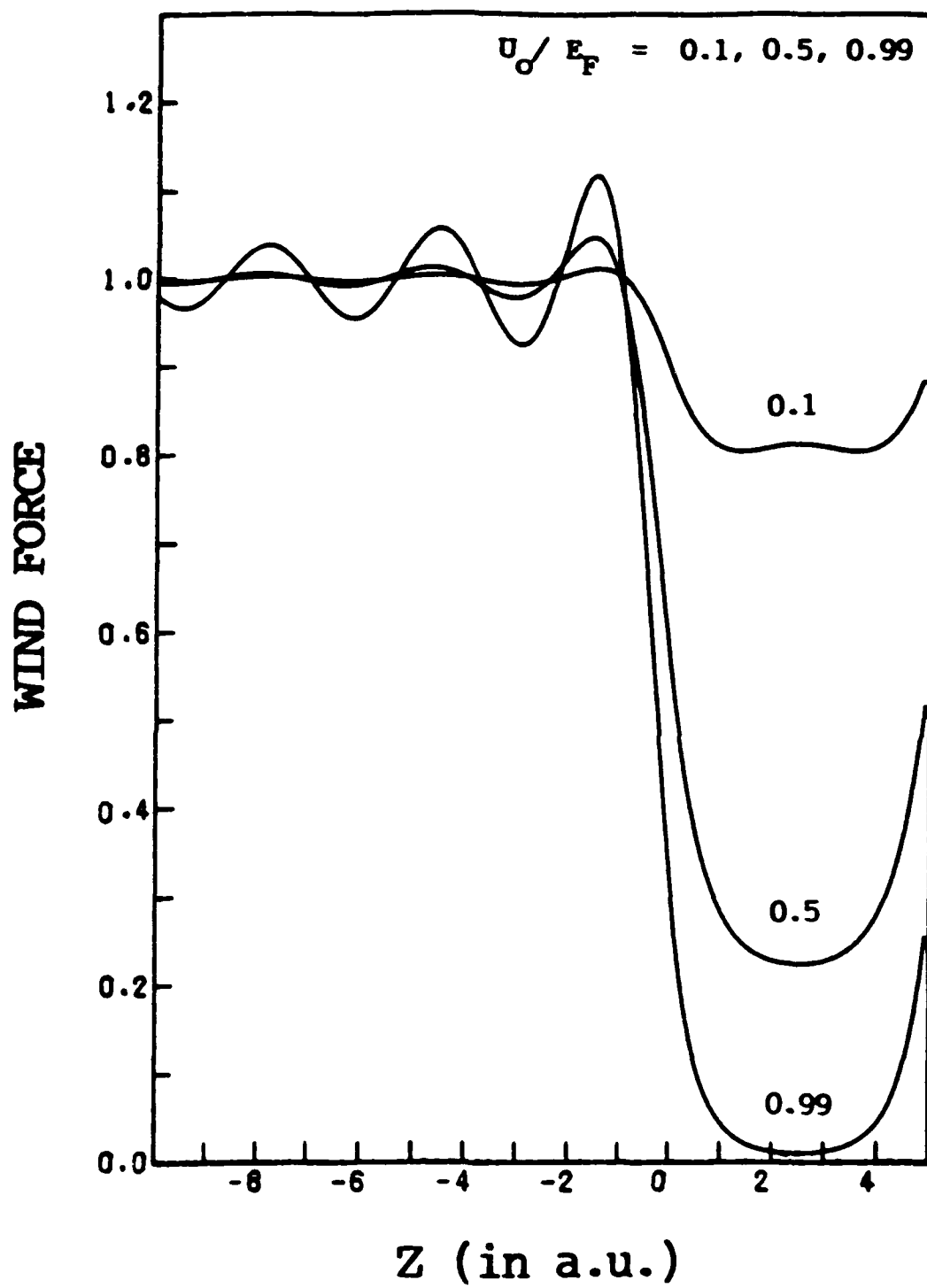
Figure 1a.   <u>Wind force near a grain boundary</u>.
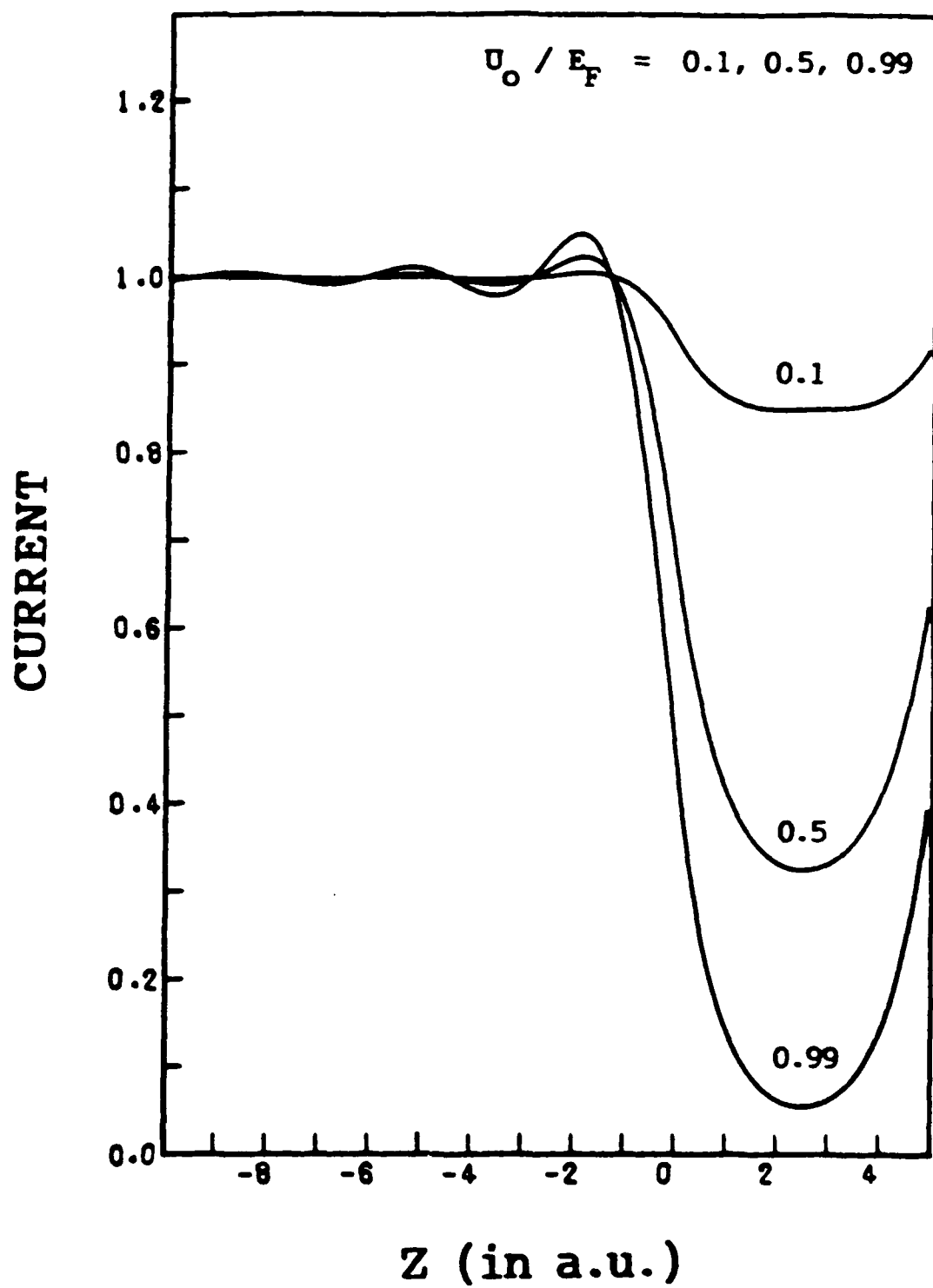
Figure 1b   <u>Current density near a grain boundary</u>.
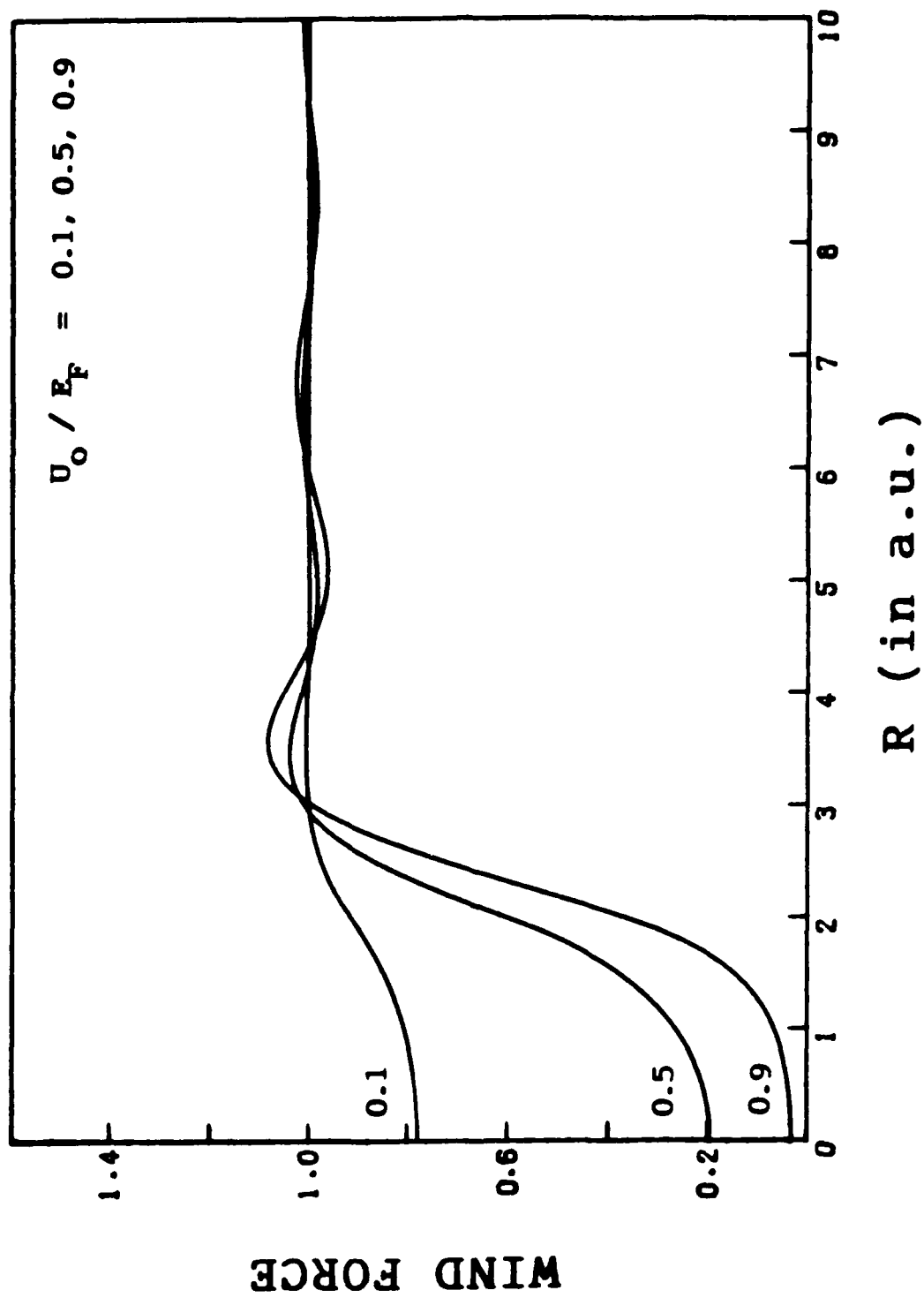
Figure 2a   Wind force near a dislocation.
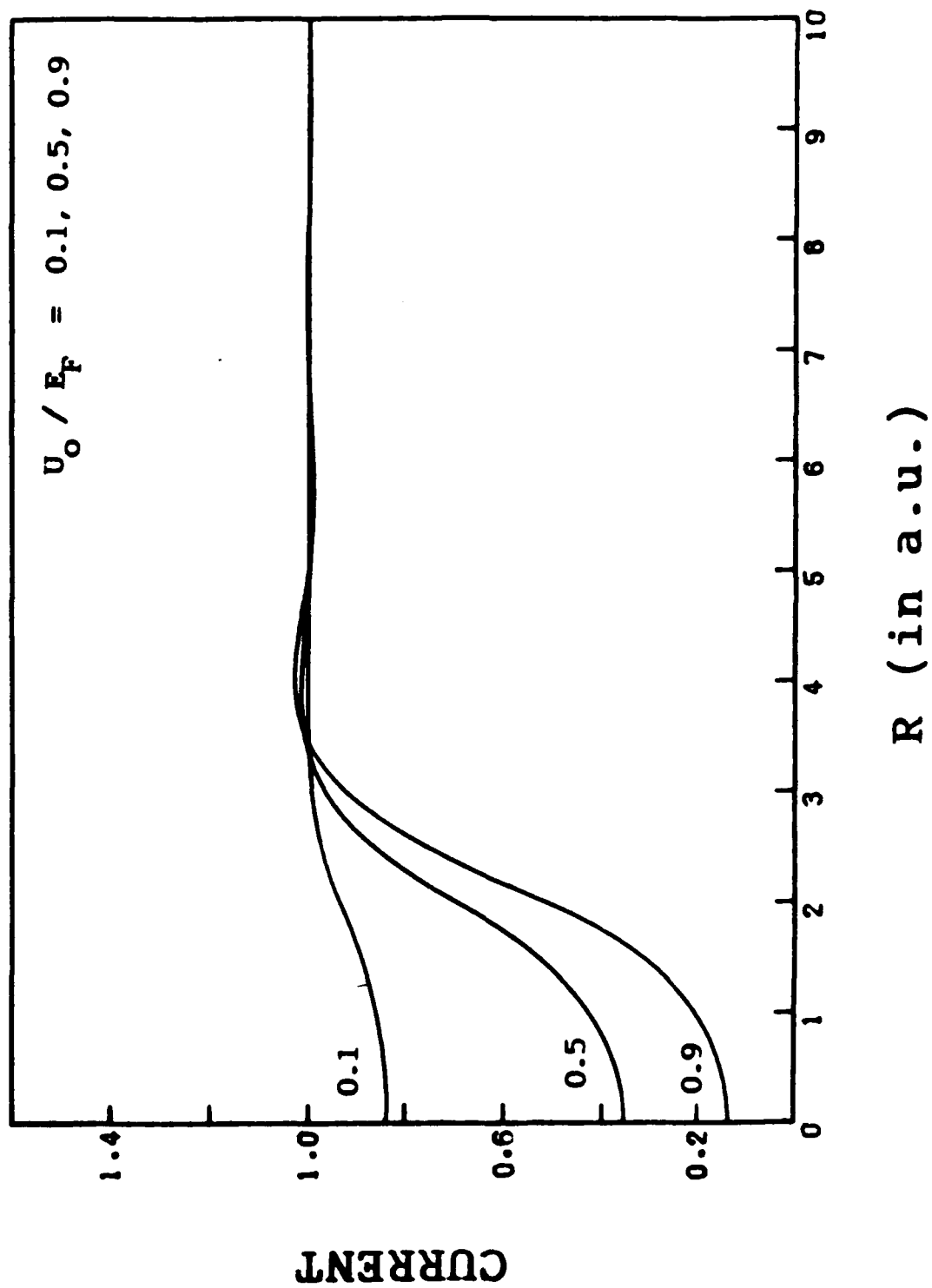
Figure 2b   Current density near a dislocation.

40
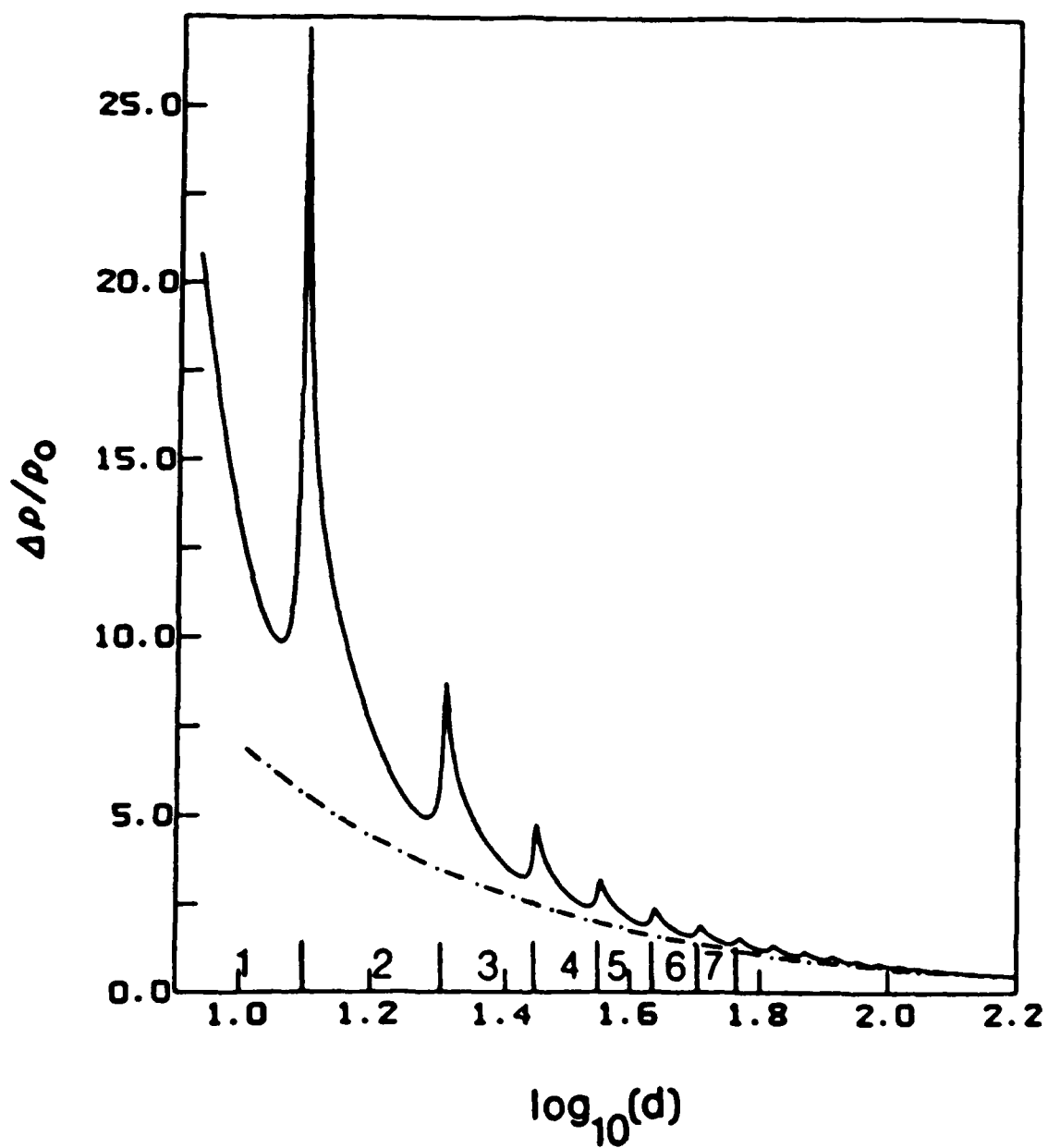
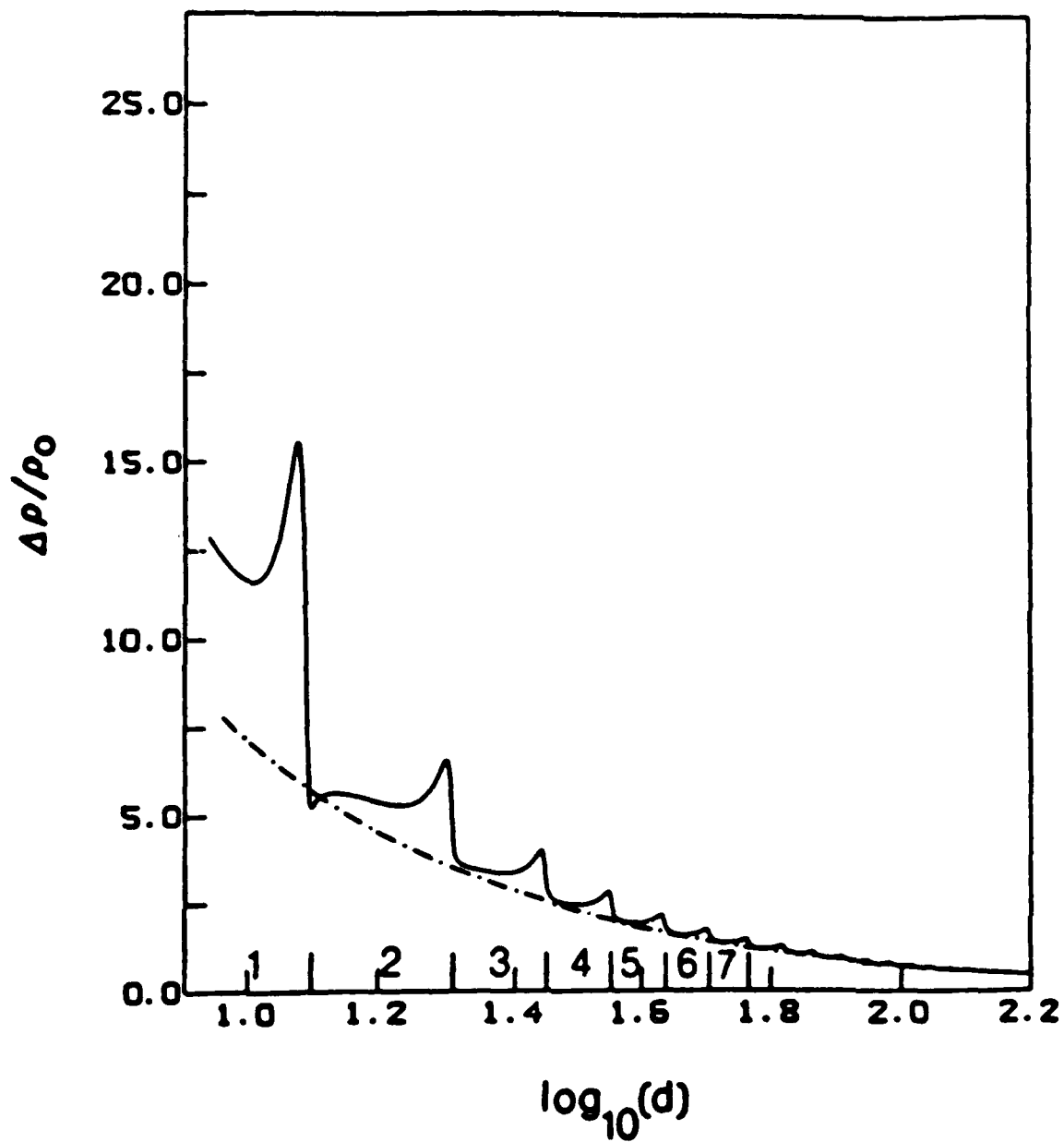Figure 3a   Impurity resistivity vs. film thickness ($\delta = 30^O$).

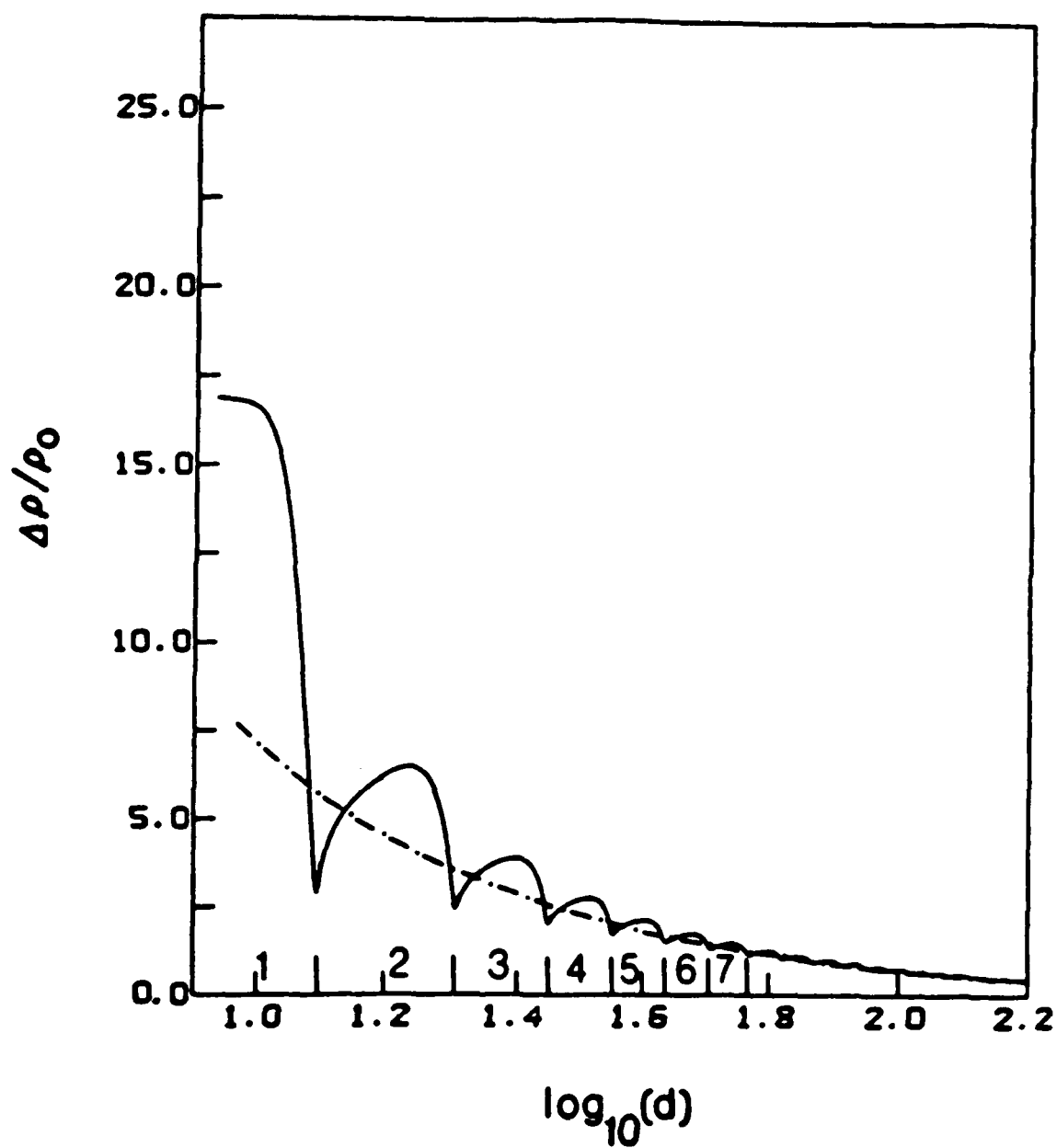Figure 3b   Impurity resistivity vs. film thickness ($\delta = 60^O$).

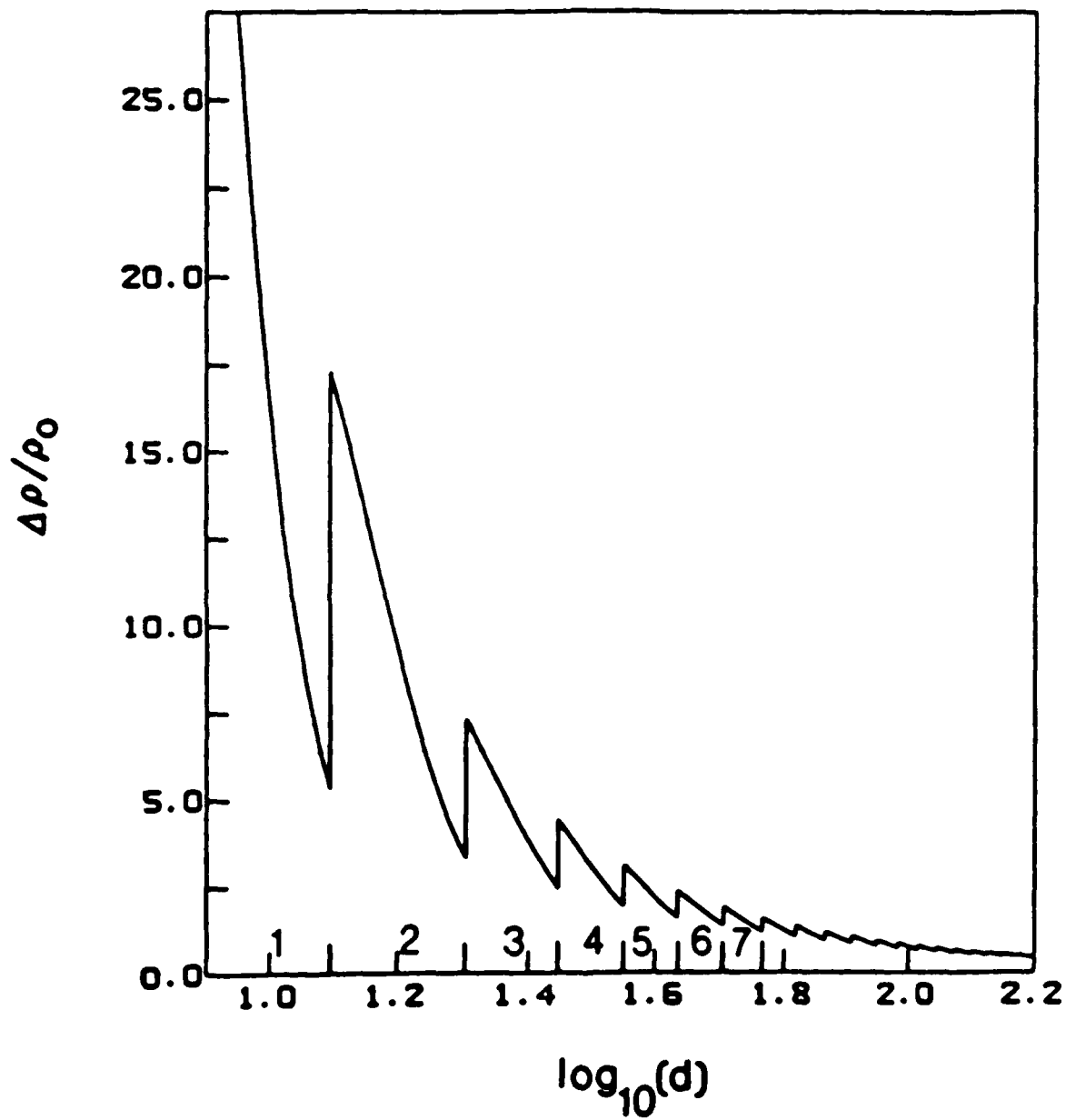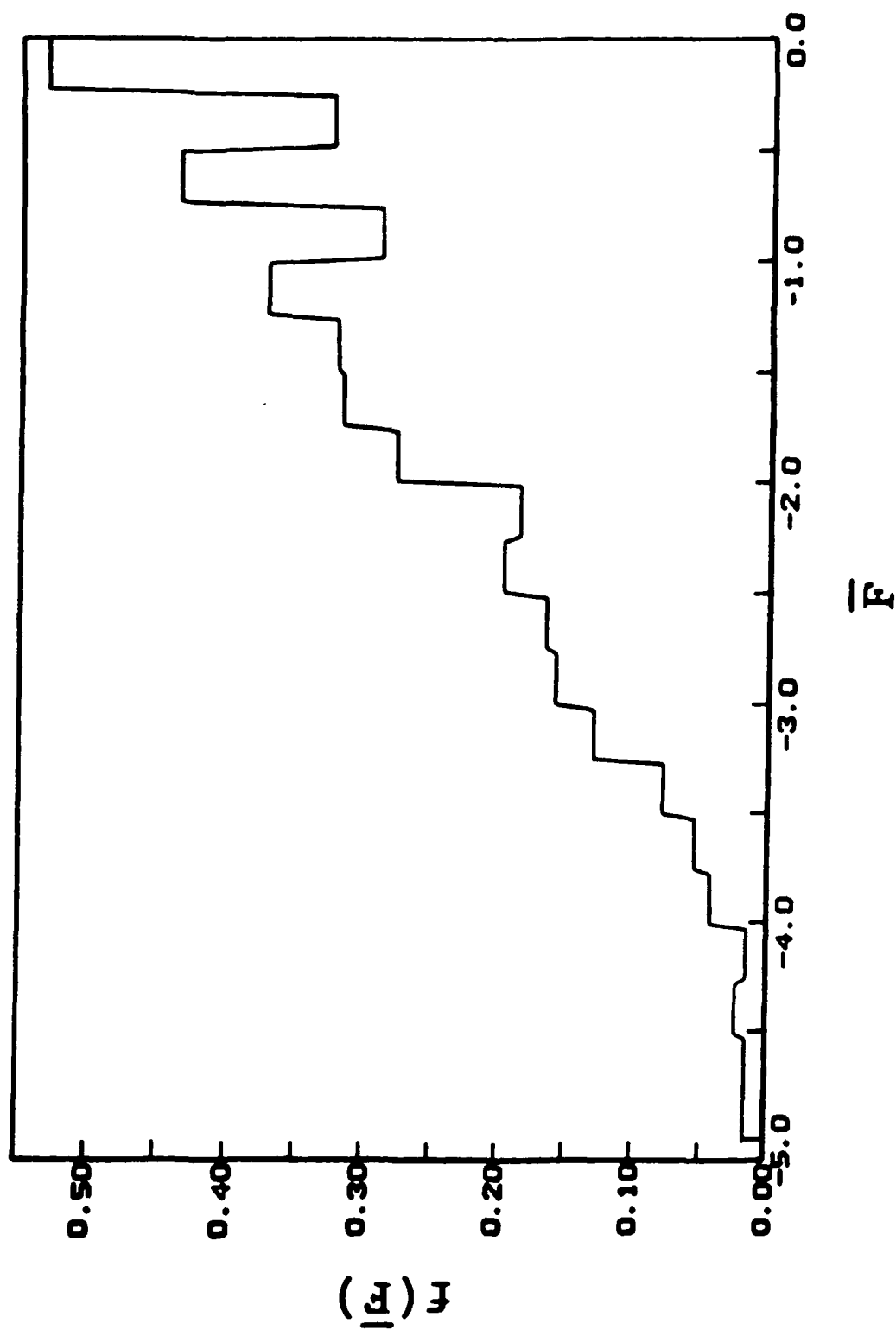Figure 3c   Impurity resistivity vs. film thickness ($\delta = 90^{O}$).

Figure 3d   Impurity resistivity vs. film thickness (Born-Approximation).

Figure 4a   Distribution for average wind force in a 1-d system.
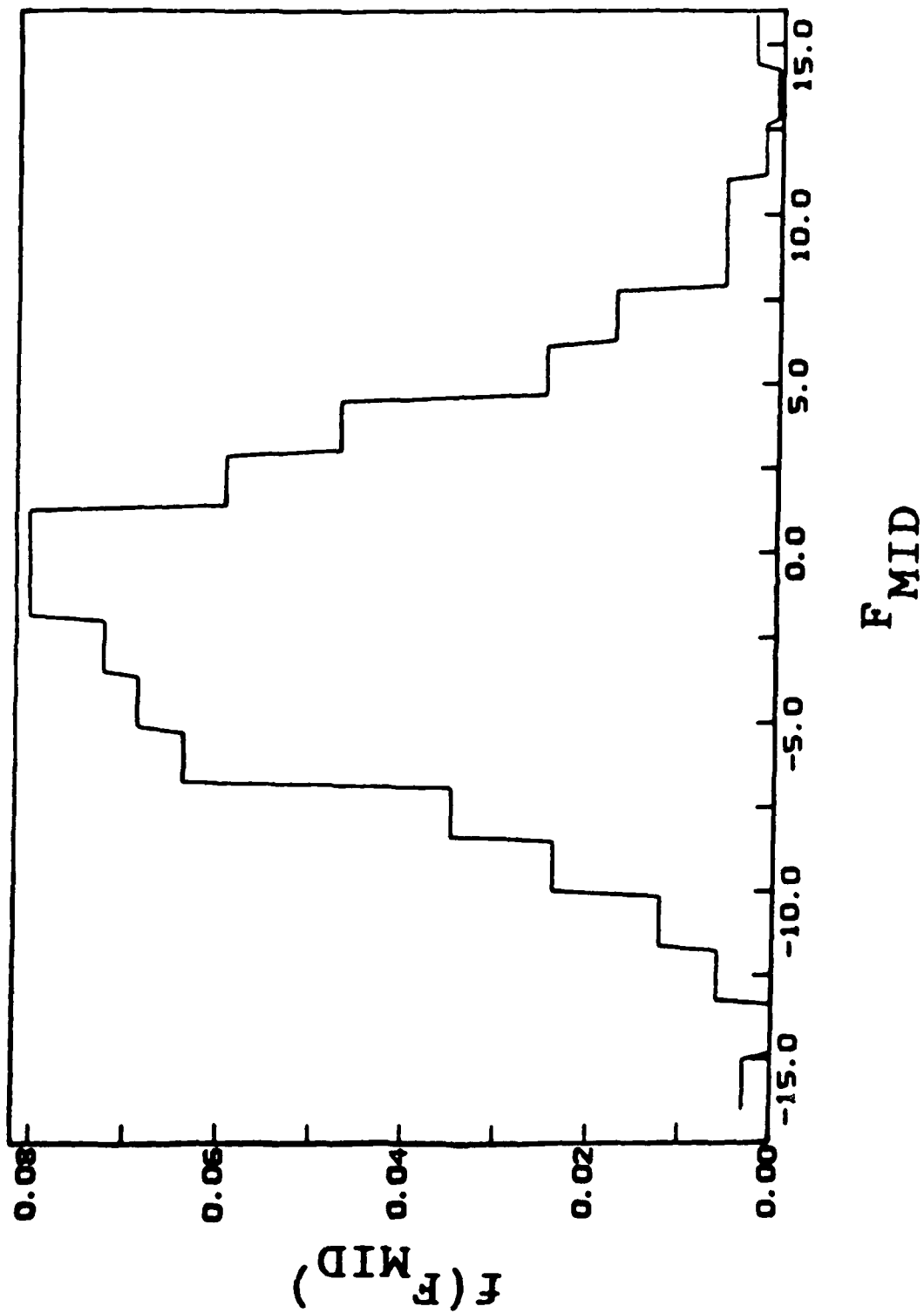
Figure 4b   *Distribution for wind force on central impurity in a 1-d system.*
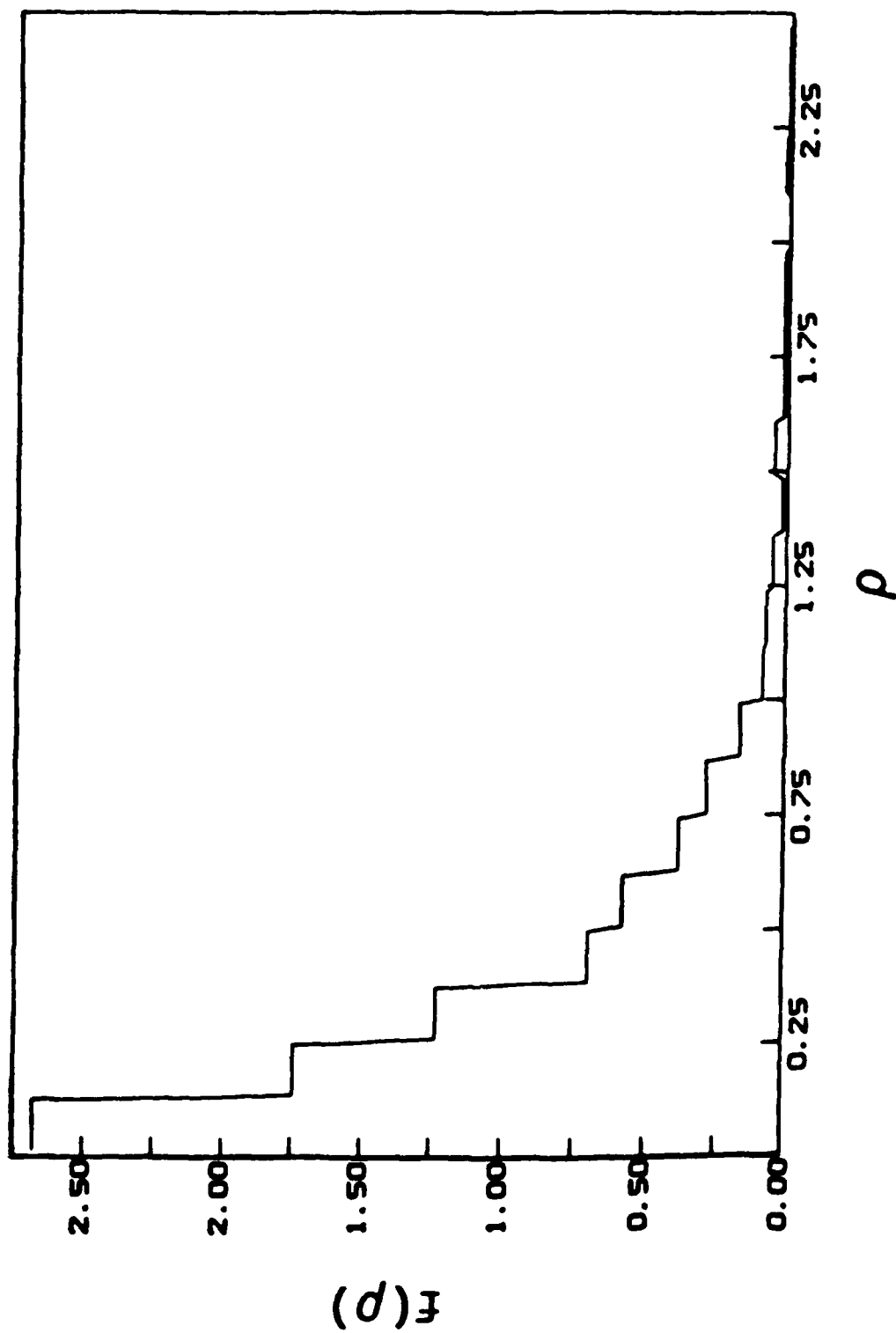
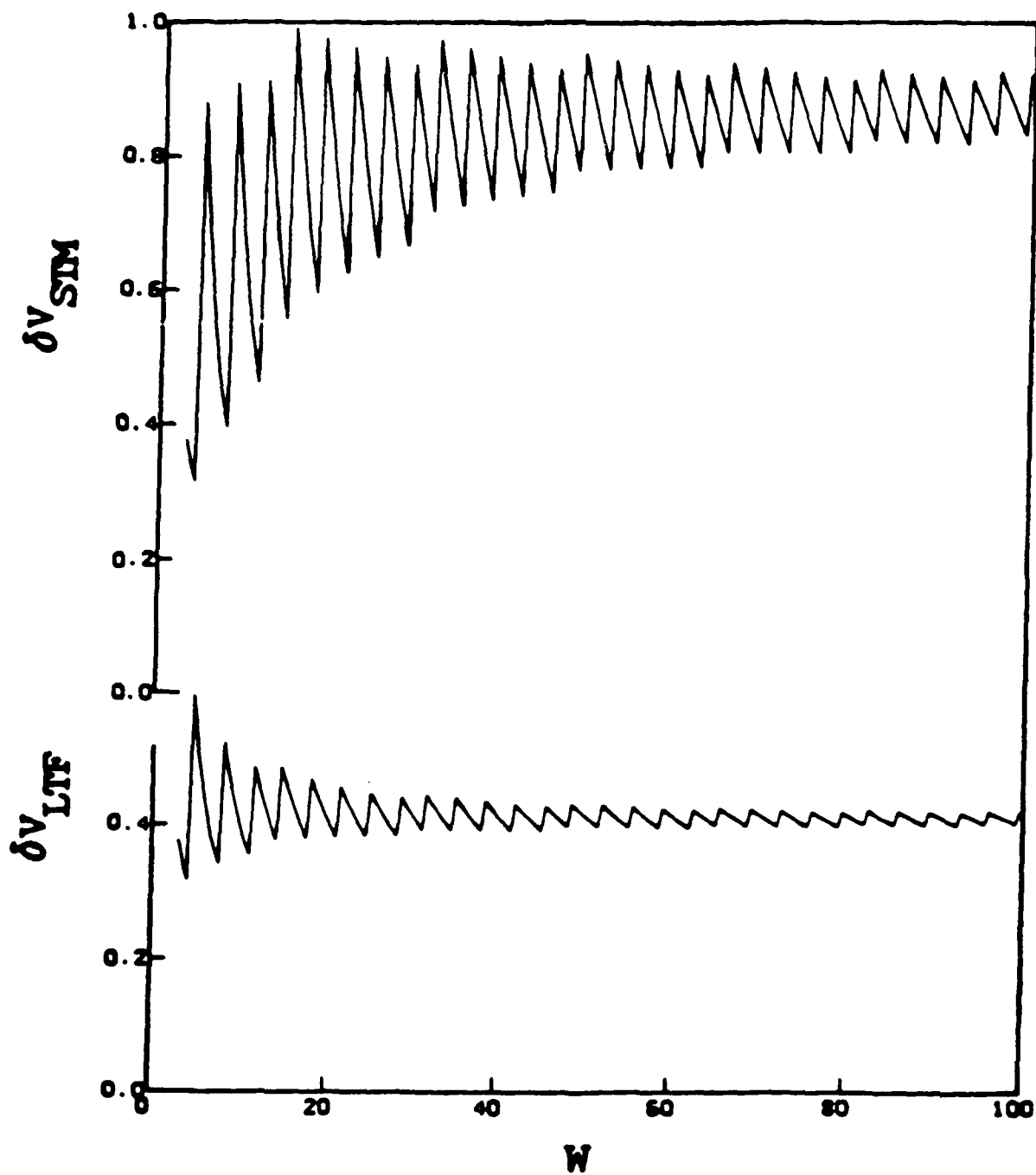Figure 4c   Distribution for resistivity in a 1-d system.
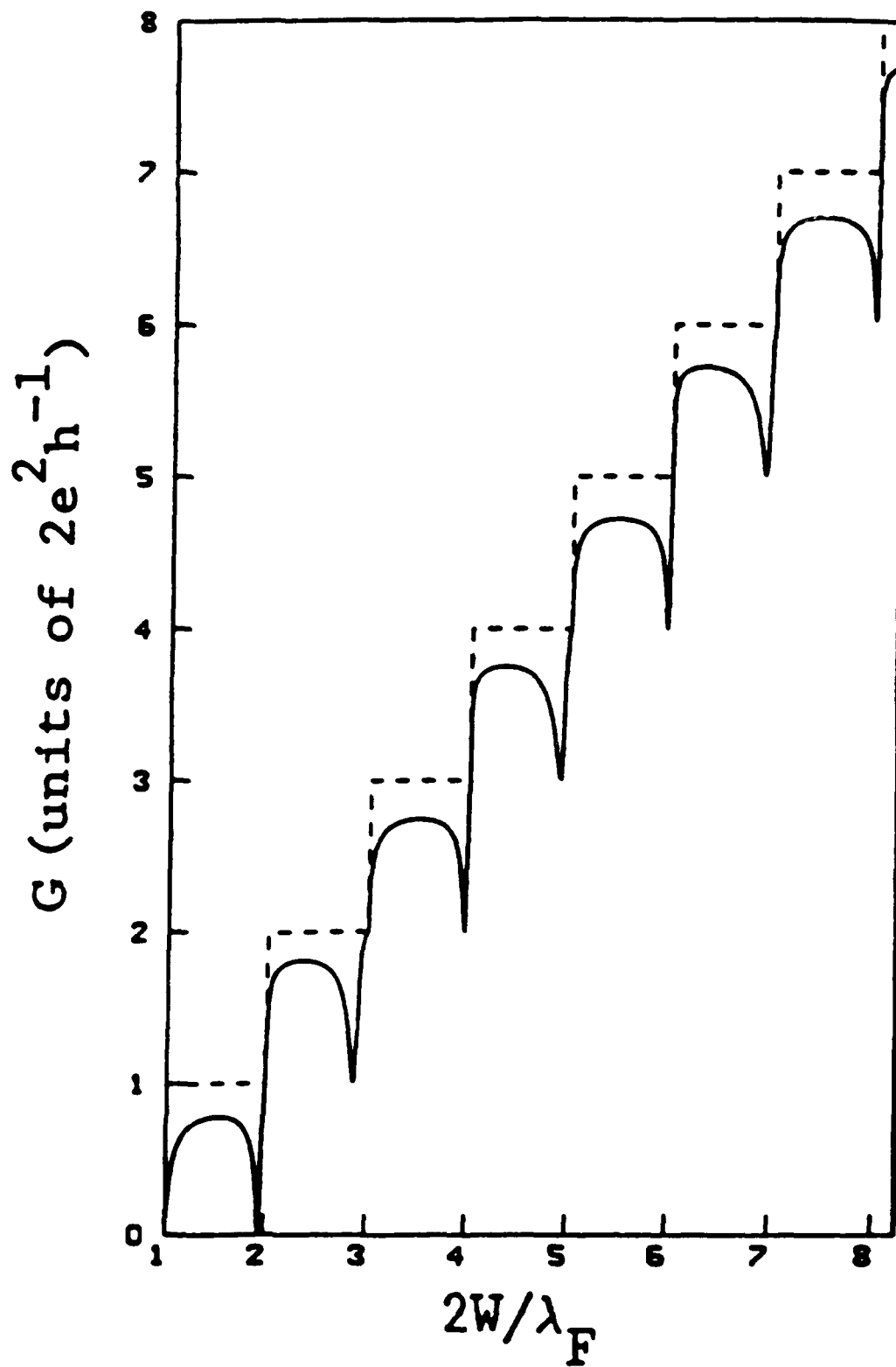
Figure 5   STM voltage and LTF voltage vs. film thickness W.

Figure 6   Conductance vs. channel width.